

STUDY OF VOLTAGE STABILITY USING INDICES

A Project Report

Submitted in partial fulfilment of the requirements

for the award of the degree of

BACHELOR OF TECHNOLOGY AND MASTER OF TECHNOLOGY

in

ELECTRICAL ENGINEERING

ABDUSSALAM TK

(EE12B067)

Under the guidance of

Dr. K. Shanti Swarup



Department of Electrical Engineering

Indian Institute of Technology- Madras

Chennai- 600036

May 2017

CERTIFICATE

This is to certify that the thesis entitled “**Real time voltage stability analysis using PMUs**” submitted by **Abdussalam TK, (EE12B067)** to the **Indian Institute of Technology Madras** in partial fulfilment of the requirements for the award of the degree in **Bachelor of Technology and Master of Technology in Electrical Engineering** is a bona-fide record of the project work done by him under my supervision.

Place: Chennai

Date:

Dr. K. Shanti Swarup
(Project Guide)

Professor

Dept. of Electrical Engineering

IIT-Madras, Chennai - 600 036

ACKNOWLEDGEMENT

It gives me great pleasure to express my sincere and heartfelt gratitude to **Dr. K. Shanti Swarup** for his excellent guidance, motivation and constant support throughout my project. I consider myself extremely fortunate to have had a chance to work under his supervision. In spite of his hectic schedule he was always approachable and took his time to discuss problems and give his advice and encouragement. I am also grateful for the laboratory facilities provided by him in the Department of Electrical Engineering, which facilitated my work.

Abdussalam TK
EE12B067

ABSTRACT

Keywords: Phasor Measurement Unit, Synchrophasor, Voltage Stability, Voltage Stability Index.

Power system voltage collapse is a very complex subject that has been challenging the power system engineers in the past two decades. As interconnections between independent power systems were found to be economically attractive, the complexity of the voltage collapse increased. When a bulk power transmission network is operated close to the voltage to the voltage stability limit, it becomes difficult to control the reactive power demand for the system. As a result, the system voltage stability will be affected, which if undetected may lead to voltage collapse. Since the introduction of phasor measurement units (PMU) in 1988, wide area measurement systems (WAMS) and wide area measurement system based monitoring, protection and control (WAMPAC) have gained significant importance in power industry. Synchronized phasor measurement technology is capable of directly measuring power system variables (voltage and current phasors) in real time, synchronized to within a millisecond. This thesis discusses the applicability of three voltage stability indices based on PMU data. Three test cases were conducted on the IEEE 14 bus system using PowerFactory software. The three indices were analysed and compared each other. From the simulation results it is clear that the indices can predict voltage collapse. Indices can also provide details about locations within the system that can contribute to instability. The performances of these indices are coherent to each other regarding to voltage stability of the system.

TABLE OF CONTENTS

ACKNOWLEDGEMENT.....	i
ABSTRACT.....	ii
LIST OF TABLES.....	v
LIST OF FIGURES.....	vi
1. INTRODUCTION.....	1
1.1 Motivation and Objectives.....	2
1.2 Organisation of the Thesis.....	3
2. VOLTAGE STABILITY.....	5
2.1 Power System Stability.....	5
2.2 Voltage Stability.....	7
2.3 Causes of Voltage Instability.....	10
2.4 Voltage Stability Analysis.....	12
3. VOLTAGE STABILITY ANALYSIS.....	21
3.1 Synchrophasors and Phasor Measurement Units.....	21
3.2 Thevenin Equivalent for Large Power Systems.....	24
3.3 VSI based on Maximum Power Transfers.....	28
3.4 VOLTAGE COLLAPSE PROXIMITY INDICATOR.....	29
3.5 Power Transfer Stability Index.....	30
4. TEST SYSTEM AND TEST CASES.....	32
4.1 DigSilent PowerFactory.....	32
4.2 IEEE 14 Bus System.....	33
4.3 Test Cases.....	36

4.4 Synopsis of Indices.....	37
5. SIMULATION RESULTS.....	41
5.1 Case 1: Increasing Load Demand.....	41
5.2 Case 2: Increasing Load Reactive Power Demand.....	46
5.3 Case 3: Line Outage.....	50
5.4 Voltage Collapse Predictability from Indices.....	50
5.5 Weakest Bus.....	51
5.6 Stability Margin.....	53
6. CONCLUSION AND FUTURE SCOPE.....	54
 APPENDIX A: MATLAB CODE	

LIST OF TABLES

2.1	Voltage Collapse Incidents.....	12
4.1	IEEE 14 Bus System- Generator Data.....	34
4.2	IEEE 14 Bus System- Load Data.....	35
4.3	IEEE 14 Bus System- Line Data.....	35
4.4	Summary of Selected Indices.....	37
5.1	Load factor with corresponding Total System Load.....	41
5.2	VSI for different Load factors (Case 1).....	42
5.3	VCPI for different Load factors (Case 1).....	43
5.4	PTSI for different Load factors (Case 1).....	43
5.5	VSI for Case 2.....	46
5.6	VCPI for Case 2.....	47
5.7	PTSI for Case 2.....	47
5.8	Values of Indices Before and After Line Tripped.....	50
5.9	Indices before Collapse: Case 1 and Case 2.....	51
5.10	Comparison of Rankings between the Indices: First Load Increase.....	52
5.11	Comparison of Rankings between the Indices: Final Load Increase.....	52

LIST OF FIGURES

2.1	Power system stability classifications.....	5
2.2	A simple Two Bus System.....	16
2.3	PV curves.....	17
2.4	Power Margin.....	18
2.5	QV curves.....	19
3.1	Phasor representation of waveforms.....	22
3.2	Partition of Interconnected Power System.....	24
3.3	External System Equivalent.....	25
3.4	Simplified Thevenin Network.....	27
3.5	A simple power system to determine VSI.....	28
3.6	Simple two bus Thevenin Equivalent system.....	30
4.1	IEEE 14 Bus Test System.....	34
4.2	Algorithm for Computing VCPI.....	38
4.3	Algorithm for Computing VSI.....	39
4.4	Algorithm for Computing PTSI.....	40
5.1	VSI for Load Buses 9, 10 and 14 (Case 1).....	44
5.2	VCPI for Load Buses 9, 10 and 11 (Case 1).....	45
5.3	PTSI for Load Buses 9, 10 and 14 (Case 1).....	45
5.4	VSI for Case 2: Bus 9, 10 and 11.....	48
5.5	VCPI for Case 2: Bus 9, 10 and 11.....	49
5.6	PTSI for Case 2: Bus 9, 10 and 11.....	49

CHAPTER 1

INTRODUCTION

During the last few years, the restricted growth of electric transmission system and increasingly higher power demands have forced utilities to operate power networks relatively close to their transmission limits. As system load increases, voltage magnitudes throughout a power network will slowly decline and continuing increase in loads may eventually drive a power system to a state of voltage instability and may cause a voltage collapse. Recent blackouts around the world are mainly due to voltage collapse occurring in stressed power systems which are associated with low voltage profiles, heavy reactive power flows, inadequate reactive support and heavily loaded systems. The consequences of voltage collapse often require long system restoration while large groups of customers are left without supply for extended periods of time. Therefore, the study of voltage instability and voltage collapse is still a major concern in power systems. The root causes of these blackouts were among others a shortage of reliable real-time data, no time to take decisive and suitable remedial action against unfolding events and a lack of properly automated and coordinated controls to take immediate action to prevent cascading.

Because power systems are operating closer to their limits, voltage stability assessment and control, although not a new issue, is now receiving a special attention. The study of voltage stability can be analysed under different approaches, but specially, the assessment of how close the system is to voltage collapse can be very useful for operators. This information on the proximity of voltage instability can be given through Voltage Stability Indices. These indices can be used online to enable the operators to take action or even to automate

control actions to prevent voltage collapse from happening or offline for the designing and planning stages.

Since the introduction of phasor measurement units (PMU) in 1988 [1], wide area measurement systems (WAMS) and wide area measurement system based monitoring, protection and control (WAMPAC) [2] have gained significant importance in power industry. Synchronized phasor measurement technology is capable of directly measuring power system variables (voltage and current phasors) in real time, synchronized to within a millisecond. There are many studies on voltage stability indices including based on phasor measurements. Some comparisons between these different indices can be found in the literature, such as [3-6]. These new algorithms use voltages and currents provided by the PMU (synchronized to within a microsecond) to assess the stability of the power system.

1.1 MOTIVATION AND OBJECTIVES

Power system voltage collapse is a very complex subject that has been challenging the power system engineers in the past two decades. As interconnections between independent power systems were found to be economically attractive, the complexity of the voltage collapse increased. When a bulk power transmission network is operated close to the voltage to the voltage stability limit, it becomes difficult to control the reactive power demand for the system. As a result, the system voltage stability will be affected, which if undetected may lead to voltage collapse. Therefore, an appropriate way must be found to monitor the system and avoid system voltage collapse.

This work studies the voltage instability problem using voltage stability indices based on PMU data. Using the indices, proximity to voltage collapse and the voltage weak areas will

be studied. Conventional voltage stability analysis, PV and QV curve methods will be discussed in this thesis. Voltage Stability index (VSI), VOLTAGE COLLAPSE PROXIMITY INDICATOR (VCPI) and Power Transfer Stability Index (PTSI) are the three indices used in this work. Analysis and comparison of these three indices based on simulated PMU data will be conducted and discussed. Three test cases, increasing load demand at constant power factor, increasing reactive power demand and line outage will be created to demonstrate the application of indices in voltage stability analysis. Results will reveal their overall effectiveness in its application to the voltage stability problem. IEEE 14 bus system is used for this work. An attempt to determine the weakest will be done by considering the indices values. All the test case simulations will be done using Powerfactory software and the indices will be implemented using Matlab.

1.2 ORGANISATION OF THE THESIS

The thesis is organised into 6 chapters.

Chapter 1 gives an introduction of the work, motivation and objectives of the work.

Chapter 2 explains Voltage Stability, causes of Voltage Instability, Voltage Stability Analysis and PV and QV curve methods.

Chapter 3 explains about Synrophasors and Phasor Measurement Units. Methodology to find Thevenin equivalent for large power systems is explained. Explains three indices proposed in literature and their methods used to evaluate voltage stability of power systems.

Chapter 4 provides a detailed description of IEEE 14 bus test system. Test cases for analysing the indices are discussed. Algorithms for computing the indices are also explained in this chapter.

Chapter 5 provides simulation results for the test cases. The results are analysed and discussed to verify the proposed indices on their applicability to determine voltage stability.

Chapter 6 provides a review of the results and its inferences are stated with recommendations for future work.

Matlab codes developed for this work are given in the **Appendix**.

CHAPTER 2

VOLTAGE STABILITY

2.1 POWER SYSTEM STABILITY

Power system stability is the ability of an electric power system, for a given initial operating condition, to regain a state of operating equilibrium after being subjected to a physical disturbance, with most system variables bounded so that the system remains intact [7]. Due to the various types of disturbances introduced, power system stability can be further classified into appropriate categories. These system variables are categorized, as shown in figure 2.1, based on disturbance magnitude and time response.

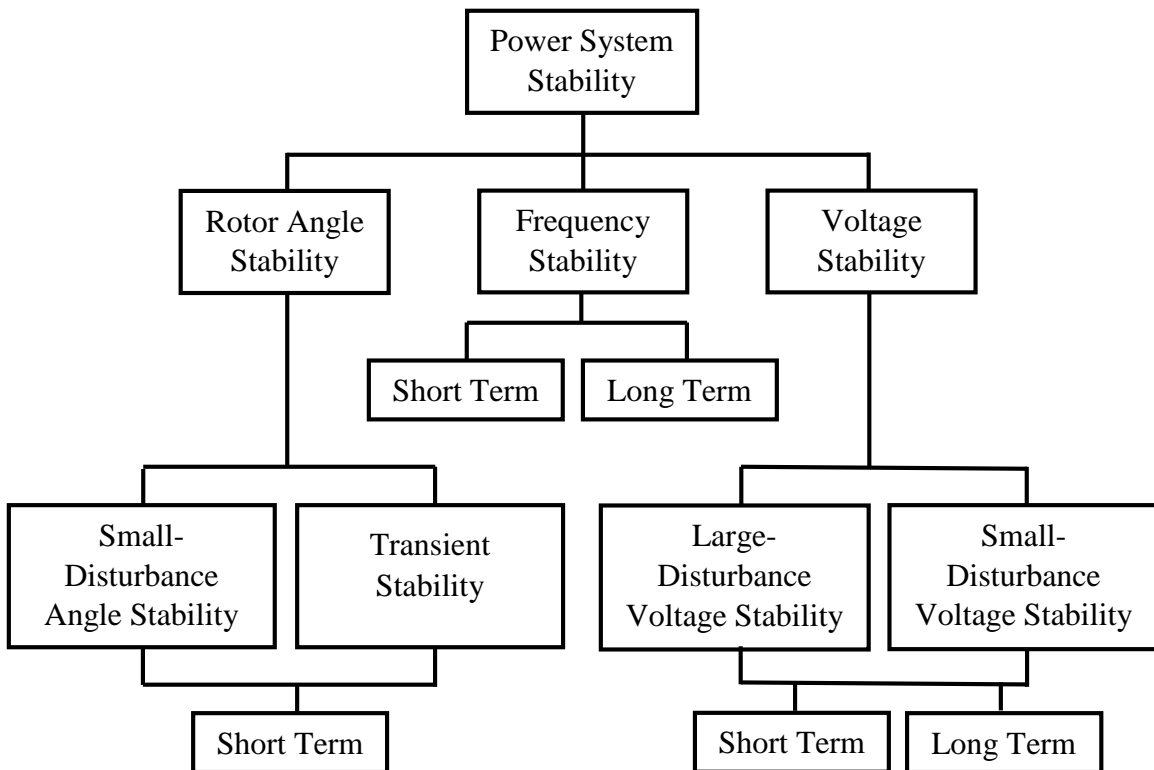


Figure 2.1 Power system stability classifications [8]

In any given situation, one form of instability can possibly lead to another form. However, distinguishing between different forms can provide convenience in identifying the underlying causes of instability, applying an appropriate analysis and ultimately taking corrective measures to return the system to a stable operating point.

2.1.1 Rotor Angle Stability

The rotor angle stability is defined as the ability of interconnected synchronous machines to remain in synchronism under normal operating conditions and after being subjected to a disturbance. In general, the total active electrical power fed by the generators must always be equal to the active power consumed by the loads; this includes also the losses in the system. This balance between the load and generation can be associated to the balance between the generator input, or mechanical torque, and the generator output, or electrical torque. A disturbance to the system can upset this equilibrium, which results in the acceleration or deceleration of the rotors of the generators. If one generator temporarily runs faster than another, the angular position of its rotor relative to that of the slower machine will increase. The resulting angular difference transfers a part of the load from the slow machine to the fast machine, depending on the theoretically known power angle relationship. This tends to reduce the speed difference and hence the angular separation. A further increase in angular separation results in a decrease in power transfer, which can lead to further instability.

2.1.2 Frequency Stability

Frequency stability refers to the ability of a power system to maintain steady frequency following a severe system upset, resulting in a significant imbalance between generation and load. It depends on the ability to maintain or restore equilibrium between system

generation and load, with minimum unintentional loss of load. Instability that may result occurs in the form of sustained frequency swings. A typical cause for frequency instability is the loss of generation causing the overall system frequency to drop. Generally, frequency stability problems are associated with inadequacies in equipment responses, poor coordination of control and protection equipment, or insufficient generation reserve.

2.1.3 Voltage Stability

The third power system stability problem is the voltage stability and is elaborated in section 2.2. Further analyses and the method proposed in the framework of this thesis are focused only on this last type of power system stability.

2.2 VOLTAGE STABILITY

Voltage stability refers to the ability of a power system to maintain steady voltages at all buses in the system after being subjected to a disturbance from a given initial operating condition [8].

The voltage stability definitions according to [8] are as follows:

A power system at a given operating point is small-disturbance voltage stable if, after a small disturbance, voltages near loads are similar or identical to pre-disturbance values.

A power system at a given operating point and subject to a given disturbance is voltage stable if voltages near loads approach post disturbance equilibrium values.

A power system at a given operating point and subject to a given disturbance undergoes voltage collapse if post-disturbance equilibrium voltages are below acceptable limits. Voltage collapse may be system wide or partial.

Power system is voltage stable if voltages after a disturbance are close to voltages at normal operating condition. A power system becomes unstable when voltages uncontrollably

decrease due to increment of load, decrement of production, weakening of voltage and/or outage of equipment (generator, line, transformer, bus bar, etc...). Voltage control and instability are local problems. However, the consequences of voltage instability may have a widespread impact. Voltage collapse is the catastrophic result of a sequence of events leading to a low-voltage profile suddenly in a major part of the power system.

Voltage stability can also called “load stability”. A power system lacks the capability to transfer an infinite amount of electrical power to the loads. The main factor causing voltage instability is the inability of the power system to meet the demands for reactive power in the heavily stressed systems to keep desired voltages. When reactive losses increase, the voltage magnitude decreases. Therefore, as the real power flow increases the voltage magnitudes tend to decrease. There is a point that the system can no longer support the real power flow on the lines and maintain a stable voltage. Thus the voltage collapses.

The power system lacks the capability to transfer power over long distances or through high reactance due to the requirement of a large amount of reactive power at some critical value of power or distance. Transfer of reactive power is difficult due to extremely high reactive power losses, which is why the reactive power required for voltage control is produced and consumed at the control area.

2.2.1 Classifications

Voltage stability can be classified, as seen in Figure 2.1, in two ways: according to the time frame of their evolution (long-term or short-term voltage stability) or to the disturbance (large disturbance or small disturbance voltage stability).

Short-term (transient) voltage stability involves a fast phenomenon with a timeframe in the order of fractions of a second to a few seconds. Short-term stability problems are usually related to the rapid response of voltage controllers such as generator automatic voltage regulator (AVR) and power electronics converters like flexible AC transmission system (FACTS) or high voltage DC (HVDC) links.

Long-term voltage stability involves slower acting equipment such as load recovery by the action of on-load tap changer or through load self-restoration and delayed corrective control actions such as shunt compensation switching or load shedding. The study period of interest may extend to several or many minutes. The modelling of long-term voltage stability requires consideration of transformer tap changers, characteristics of static loads, manual control actions of operators and automatic generation control.

For analysis purposes, it is also useful to classify voltage stability into small and large disturbances:

Large-disturbance voltage stability refers to the system's ability to maintain steady voltages following large disturbances such as system faults, loss of generation, or circuit contingencies and the period of interest may extend from a few seconds to tens of minutes. Large-disturbance voltage stability can be studied using non-linear time domain simulations in the short-term time frame and load flow analysis in the long-term time frame.

Small-disturbance voltage stability refers to the system's ability to maintain steady voltages when subjected to small perturbations such as incremental changes in system load [9]. Usually, the analysis of small-disturbances is done in steady state with the power system linearized around an operating point.

In summary, in any given situation, each form of stability are closely associated with one another, and thus one form of instability can possibly lead to another form. Distinguishing between these different forms can provide convenience in identifying the underlying causes of instability, applying an appropriate analysis and ultimately, taking corrective measures to return the system to a stable operating point. With this in mind, the following section will provide an overview on the existing methods used to analyze voltage stability.

2.3 CAUSES OF VOLTAGE INSTABILITY

Various system aspects may cause voltage instability. Amongst the most important aspects are generators, transmission lines, and loads [10].

Generators play an important role for providing adequate reactive power support for power systems. Reactive power is produced by generators and therefore limited by the current rating of the field and armature windings. Since there are levels to how much current or heat the exciter winding can take before the winding becomes damaged, the maximum reactive power output is set using an over excitation limiter (OXL). When the OXL hits the limit, the terminal voltage is no longer maintained constant. Therefore the power transfer limit is further limited, resulting in long-term voltage instability.

Transmission networks are other important constraints for voltage stability. Under a deregulation environment where bulk power is transferred across long distances, the maximum deliverable power is limited by the transmission system characteristics. Power beyond the transmission capacity determined by thermal or stability considerations cannot be delivered.

The third major factor that influences voltage instability is system loads. Voltage instability is load driven. Following a change in the demand, the load will at first change according to its instantaneous characteristic such as, constant impedance or current. It will then adjust the current drawn from the system until the load supplied by the system satisfies the demand at the final system voltage. Similarly when there is a sudden change in system voltage, such as, following a disturbance, the load will change momentarily. It will then adjust the current and draw from the system, whatever current is necessary in order to satisfy the demand [11].

Another important load aspect is the Load Tap Changing (LTC) transformer, which is one of the key mechanisms in load restoration. In response to a disturbance, the LTC tends to maintain constant voltage level at the low voltage end. Therefore, load behavior observed at high voltage level is close to constant power, which may aggravate voltage instability problems.

2.3.1 Voltage Collapse Incidents

Voltage collapse incidents dynamics span can range from seconds to as long as tens of minutes. Since the voltage instability issue started to emerge, research efforts from the power engineering community have been dedicated to studying the voltage instability mechanism and to developing analysis tools and control schemes to mitigate the instability.

Many voltage instability incidents have occurred around the world. Table 2.1 shows some of the several known incidents happened and their time frame.

Date	Location	Time Frame
23-Sept-2003	South Sweden/Denmark	5-6 minutes
29-July-1995	Phoenix, Arizona area, USA	3 seconds
01-Dec-1987	Western France	4-6 minutes
22-Aug-1987	Western Tennessee, USA	10 seconds
23-Jul-1987	Tokyo, Japan	20 minutes
30-Nov-1986	SE Brazil, Paraguay	2 seconds
27-Dec-1983	Sweden	55 seconds
30-Dec-1982	Florida, USA	1-3 minutes
04-Aug-1982	Belgium	4.5 minutes
19-Dec-1978	France	26 minutes
22-Aug-1970	Japan	30 minutes

Table 2.1 Voltage Collapse Incidents [8]

2.4 VOLTAGE STABILITY ANALYSIS

There are two general types of voltage stability analysis method: Dynamic analysis and Steady-state analysis. Dynamic analysis typically uses time-domain simulations to solve the system differential-algebraic equations, while steady-state analysis focuses on the conventional or modified power-flow solution of a system snapshot.

2.4.1 Dynamic Voltage Stability Analysis

In dynamic analysis, all elements in a power system are modelled by algebraic and differential equations. The behaviour of the system under different changes of the system

is studied through time domain simulations. The whole power system can be expressed under set of algebraic and differential equations in general form as follows [12]:

$$\dot{x} = f(x, V) \quad (2.1)$$

$$I(x, V) = Y_{bus}V \quad (2.2)$$

Where x represents the system state vectors, V represents the bus voltage vector, I represents the current injection vector, and Y_{bus} represents the network node admittance matrix. (2.1) describes the interested dynamics of the system. (2.2) describes the network algebraic constraints. Dynamic analysis solves the system differential-algebraic equations and reveals the system response against subjected disturbance in time-domain.

Dynamic analysis can accurately replicate the actual dynamic of voltage stability, and show performance of system and individual elements. It can also capture the event and chronology leading to voltage instability. However, this method requires huge data information for modelling and expensive calculation efforts, while the degree of instability is not provided. In practice, dynamic simulation is applied in essential studies relating to coordination of protections and controls and short-term voltage stability analysis

2.4.2 Steady State Voltage Stability Analysis

Steady-state analysis only solves the algebraic equations of a specified system snapshot. Due to its computational efficiency, steady-state analysis is commonly used for bulk studies of practical power systems when voltage stability limit of various contingencies and operation conditions needs to be determined.

This thesis will focus only on steady state voltage stability analysis methods. In this section an introduction to power flow or load flow analysis and its application to voltage stability will be given in order to understand the voltage stability indices exposed in the next chapter.

2.4.2.1 Power Flow Analysis

The power-flow (load-flow) analysis involves the calculation of power flows and voltages of a transmission network for specified terminal or bus conditions [11]. The system is assumed to be balanced. Associated with each bus are four quantities: active power P , reactive power Q , voltage magnitude V , and voltage angle θ . The relationships between network bus voltages and currents can be represented by node equations. The network equations in terms of node admittance matrix can be written as:

$$\bar{I} = [Y][\bar{V}] \quad (2.3)$$

If n is the total number of nodes, \bar{I} is the vector ($n \times 1$) of current phasors flowing into the network, Y ($n \times n$) is the admittance matrix with Y_{ii} being the self-admittance of node i (sum of all the admittances of node i) and Y_{ij} being the mutual admittance between nodes i and j (negative of the sum of all admittances between nodes i and j), and \bar{V} the vector of voltage phasors to ground at node i .

Equation (2.3) would be linear if injections \bar{I} were known, but in practice, are not known for most nodes. The current at any node k is related to P , Q and V as follows:

$$I_k = \frac{P_k - jQ_k}{\bar{V}_k^*} \quad (2.4)$$

The relations between P , Q , V and I are defined by the characteristics of the devices connected to the nodes, which makes the problem nonlinear and have to solved using techniques such as Gauss-Seidel or Newton-Raphson method.

The Newton-Raphson method is an iterative technique for solving nonlinear equations. Using this method, the model can be linearized around a given point the following way:

$$\begin{bmatrix} \Delta P \\ \Delta Q \end{bmatrix} = \begin{bmatrix} \frac{\partial P}{\partial \theta} & \frac{\partial P}{\partial V} \\ \frac{\partial Q}{\partial \theta} & \frac{\partial Q}{\partial V} \end{bmatrix} \begin{bmatrix} \Delta \theta \\ \Delta V \end{bmatrix} \quad (2.5)$$

where $\begin{bmatrix} \frac{\partial P}{\partial \theta} & \frac{\partial P}{\partial V} \\ \frac{\partial Q}{\partial \theta} & \frac{\partial Q}{\partial V} \end{bmatrix}$ is called the Jacobian matrix, ΔP is the incremental change in bus real power, ΔQ is the incremental change in bus reactive power injection, $\Delta \theta$ is the incremental change in bus voltage angle and ΔV is the incremental change in bus voltage magnitude.

Equation (2.5) requires the solution of sparse linear matrix equations, which can be done using sparsity-oriented triangular factorization.

The Jacobian can provide useful information about voltage stability. System voltage stability is affected by both P and Q . However, at each operating point we may keep P constant and evaluate voltage stability by considering the incremental relationship between Q and V . Based on these considerations, ΔP in (2.5) is set to 0. Then,

$$\Delta Q = J_R \Delta V \quad (2.6)$$

where,

$$J_R = [J_{QV} - J_{Q\theta} J_{P\theta}^{-1} J_{PV}] \quad (2.7)$$

J_R is the reduced Jacobian matrix of the system.

Voltage stability characteristics can be determined by computing the eigenvalues and eigenvectors of this reduced Jacobian matrix defined by (2.7). Given an eigenvalue λ_i of the i_{th} mode of the Q-V response, if $\lambda_i > 0$, then the modal voltage and modal reactive power are along the same direction which yields to a voltage stable system. If $\lambda_i < 0$, the modal voltage and modal reactive power are along opposite directions which indicates an unstable system. The magnitude of λ_i determinates the degree of stability. When $\lambda_i=0$, voltage collapses because any change in the modal reactive power causes an infinite change in the modal voltage.

In conclusion, the Jacobian matrix allows defining the voltage collapse point as a system loadability limit in which the minimum magnitude of the eigenvalues of the power flow Jacobian matrix is zero.

2.4.2.2 PV and QV curves

PV and QV curves [8] are two traditional power flow methods widely used for illustrating voltage instability phenomenon. A simple example is given using PV and QV curves.

The simplified two-bus model in Figure 2.2 considers a constant voltage source of magnitude E and a purely reactive transmission impedance jX .

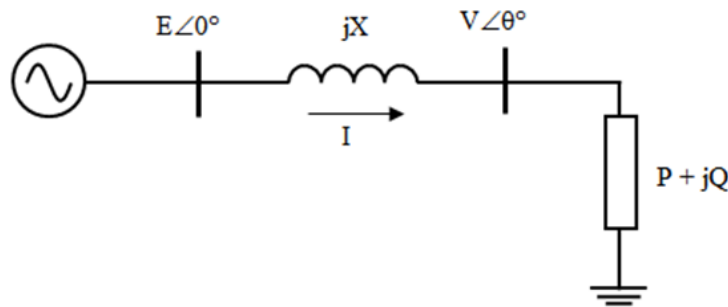


Figure 2.2 A simple Two Bus System

Using the load flow equations:

$$P = -\frac{EV}{X} \sin\theta \quad (2.8)$$

$$Q = -\frac{V^2}{X} + \frac{EV}{X} \cos\theta \quad (2.9)$$

where P is the active power consumed by the load, Q is the reactive power consumed by the load, V the load bus voltage and θ the phase angle difference between the load and generator busses. Solving (2.8) and (2.9) with respect to V , the following equation is obtained:

$$V = \sqrt{\frac{E^2}{2} - QX \pm \sqrt{\frac{E^4}{4} - X^2 P^2 - X E^2 Q}} \quad (2.10)$$

The solutions to this load voltage are often presented in PV or QV curves, also known as nose curves or voltage profiles. In Fig. 2.3, different PV curves are shown. A constant power factor, i.e., $Q=P \cdot \tan\Phi$ has been assumed for each curve.

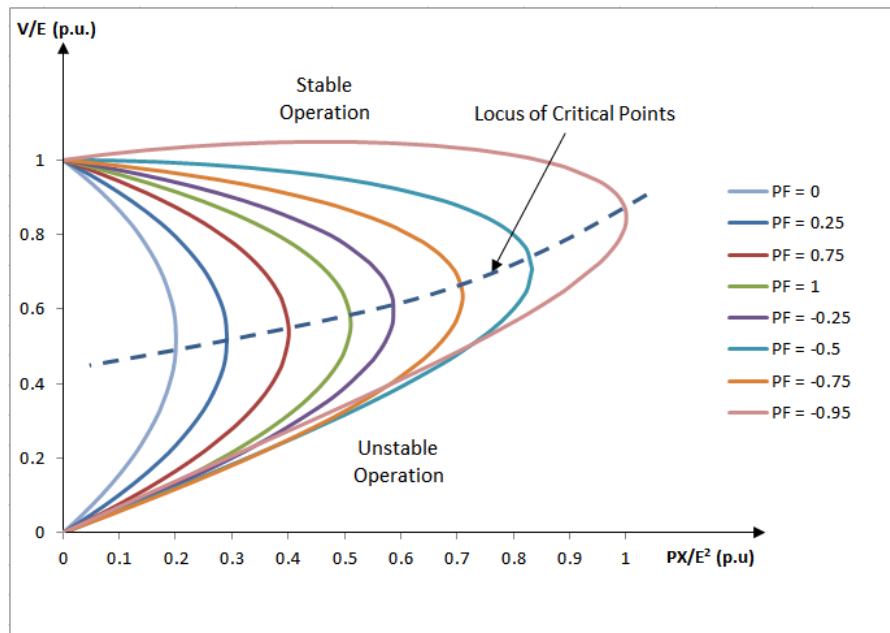


Figure 2.3 PV curves [13]

Equation (2.10) yields two solutions of voltages to any set of load flow, represented by the upper and lower parts of the PV-curve. The upper voltage solution, which is corresponding to “+” sign in equation (2.10) is stable, while the lower voltage, corresponding to “-” sign, is unstable [13]. The tip of the “nose curve” is called the maximum loading point or critical point. Operation near the stability limit is impractical and sufficient power margin, that is, distance to the limit, has to be allowed [7], as represented in Fig.2.4.

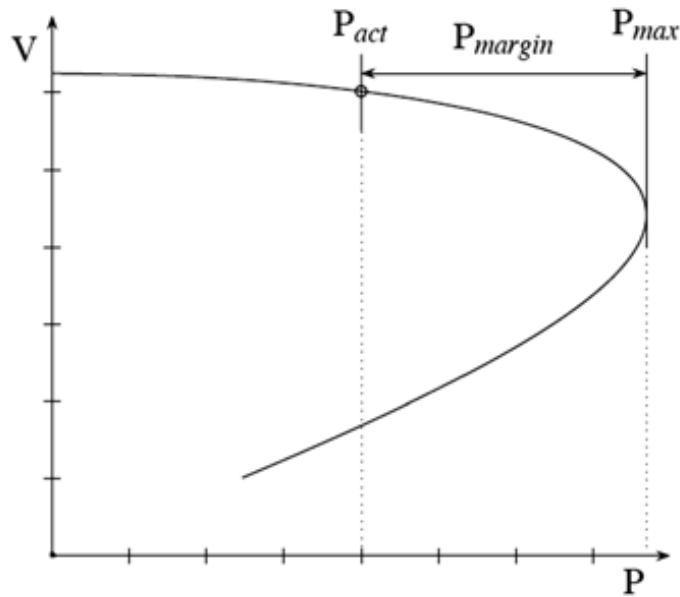


Figure 2.4 Power Margin [7]

Often, a more useful characteristic for certain aspects of voltage stability analysis is the QV curves. These can be used for assessing the requirements for reactive power compensation since they show the sensitivity and variation of bus voltages with respect to reactive power injections or absorptions.

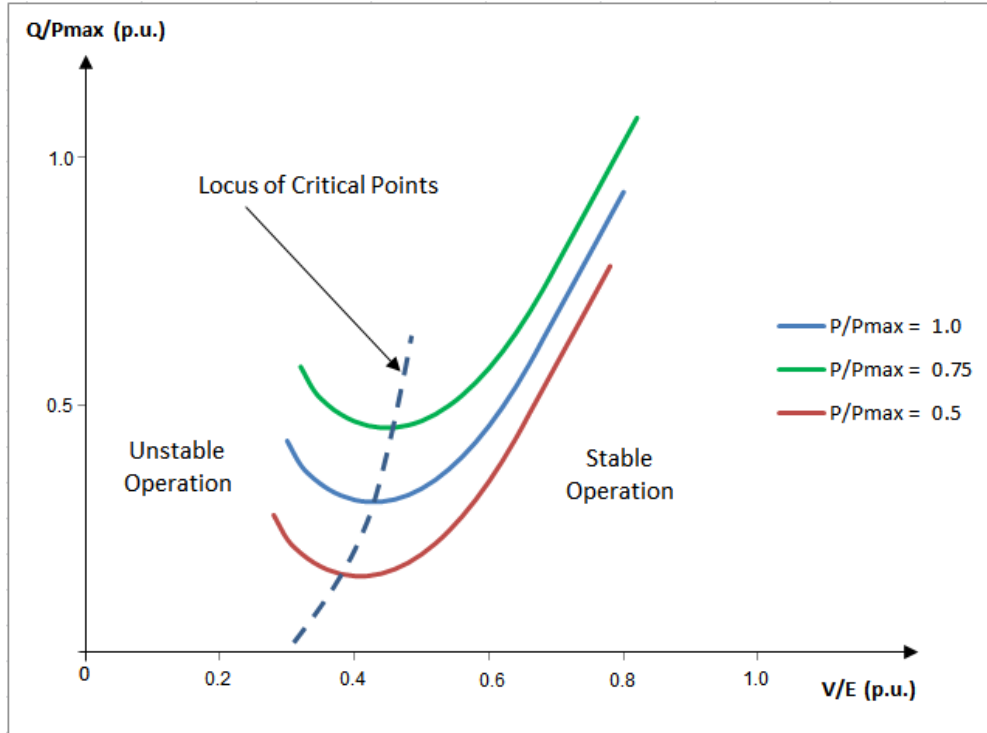


Figure 2.5 QV curves [7]

Fig. 2.6 shows Q-V curves. Similar to the P-V curves, Q-V curves have a voltage stability limit, which is the bottom of the curve, where dQ/dV is equal to zero. The right hand side is stable since an increase in Q is accompanied by an increase in V . The left hand side is unstable since an increase in Q represents a decrease in V , which is one of the instability factors that judges that a system is voltage unstable if, for at least one bus in the system, the bus voltage magnitude decreases as the reactive power injection in the same bus is increased.

In [2] it was seen that complex power systems have similar PV characteristics to those of simple radial systems such as the one in Figure 2.2. That is the reason why, PV-curves play a major role in understanding and explaining voltage stability and are widely used for its study. From a PV curve, the variation of bus voltages with load, distance to instability and

critical voltage at which instability occurs may be determined. However, it is not necessarily the most efficient way of studying voltage stability since it requires a lot of computations for large complex networks.

2.4.2.3 Voltage

Voltage is probably the most intuitive index for quantifying voltage stability. Monitoring voltage magnitudes have been a widely accepted index to initialize remedial actions such as undervoltage load shedding schemes in order to prevent voltage collapse. Typically, a voltage margin is set between 85%-90% of the nominal voltage. At this point a designated relay will trip, or dispatchers can act accordingly to drop a load in order to prevent voltage collapse.

The limitation of the voltage-based index is that it cannot quantify the distance to the voltage marginally stable point. The bus with the lowest voltage is not necessarily the one closest to the voltage collapse point. As shown in figure 2.3 - curve 4, a load bus with high reactive power compensation may not show any significant low voltage problems even if the power transfer is close to the system transmission limit and the system is close to the voltage marginally stable point.

CHAPTER 3

VOLTAGE STABILITY INDICES

In voltage stability studies, it is crucial to have an accurate knowledge of how close a power system's operating point is from the voltage stability limit. It has been observed that voltage magnitudes alone, do not give a good indication of proximity to voltage stability limit. Therefore, it is useful to assess voltage stability of a power system by means of a voltage stability index (VSI), a scalar magnitude that can be monitored as system parameters change. These indices should be capable of providing reliable information about the proximity of voltage instability in a power system and should reflect the robustness of a system to withstand outages or load increase. Likewise, these indices should be computationally efficient and easy to understand. Therefore operators can use these indices to know how close the system is to voltage collapse in an intuitive manner and react accordingly.

This chapter will provide an overview on three different PMU based voltage stability indices proposed in literature. The indices are VSI based on Maximum Power Transfers [14], VOLTAGE COLLAPSE PROXIMITY INDICATOR (VCPI) [15] and Power Transfer Stability Index [16]. This chapter also explains about Synchrophasors and phasor measurement units and Thevenin Equivalent for large power systems.

3.1 SYNCHROPHASORS AND PHASOR MEASUREMENT UNITS.

As the improvement of the transmission network becomes more complex, the need for faster clearing times, pilot protection schemes and more wide-area protection and control systems to ensure that these lines are being most utilized, has increased. Protection and

control systems must adapt to constant changes in the network. The variability on both the supply and demand side increases the importance of having wide area protection, control and monitoring systems that are secure, reliable, and simple as possible. At the heart of these new wide-area systems are time synchronized phasor data known as synchrophasors. Phasor representation of sinusoidal signals is commonly used in ac power system analysis. An AC waveform can be mathematically represented by the following equation:

$$x(t) = X_m \cos(\omega t + \varphi) \quad (3.1)$$

where:

X_m is the magnitude of the sinusoidal waveform.

ω is the angular frequency given by $\omega = 2\pi f$ and f being the frequency in Hz.

φ is the angular starting point for the waveform.

The representation of power system sinusoidal signals is commonly done in phasor notation. The waveform is then represented as $\bar{X} = X_m \angle \varphi$. The phasor representation of a sinusoid is independent of its frequency and the phase angle φ of the phasor is determined by the starting time ($t = 0$) of the sinusoid.

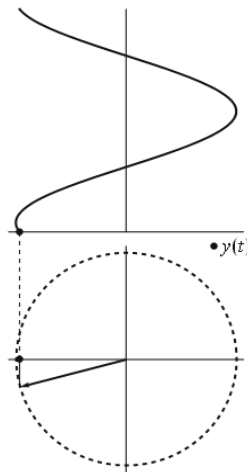


Figure 3.1 Phasor representation of waveforms

Synchronized phasor (or synchrophasor) is a complex number representation of the fundamental frequency component of either a voltage or a current, with a time label defining the time instant for which the phasor measurement is performed. The synchrophasor representation X of a signal $x(t)$ is the complex value given by:

$$X = X_r + jX_i = \left(\frac{X_m}{\sqrt{2}}\right) (e^{j\varphi}) = \left(\frac{X_m}{\sqrt{2}}\right) (\cos \varphi + j \sin \varphi) \quad (3.2)$$

where $\left(\frac{X_m}{\sqrt{2}}\right)$ is the RMS (Root Mean Square) value of the signal $x(t)$ and φ is its instantaneous phase angle relative to a cosine function at nominal system frequency synchronized to universal time coordinated (UTC).

Note that the synchrophasor standard defines the phasor referred to the RMS value. Therefore, it should be taken into account that $\sqrt{2}$ should be multiplied to the synchrophasor value when computing the actual phasor magnitude.

Phasor Measurement Units (PMUs) units are devices that provide real time measurement of positive sequence voltages and currents at power system substations. Typically the measurement windows are one cycle of the fundamental frequency. Through the use of integral GPS (Global Positioning System) satellite receiver-clocks, PMUs sample synchronously at selected locations throughout the power system. Data from substations are collected at a suitable site, and by aligning the time stamps of the measurements a coherent picture of the state of the power system is created [17]. Therefore a wide implementation of PMU offers new opportunities in power system monitoring, protection, analysis and control.

The commercialization of PMU together with high-speed communications networks makes it possible to build wide area monitoring systems (WAMSs), which takes snapshots of the power system variables within one second and provides new perspectives for early detection and prevention of voltage instability. PMU-based voltage instability monitoring can be classified in two broad categories: methods based on local measurements and methods based on the observability of the whole region [18]. The first, need few or no information exchange between the monitoring locations, while the second one requires time-synchronized measurements.

3.2 THEVENIN EQUIVALENT FOR LARGE POWER SYSTEMS

Large interconnected power systems normally can be partitioned into three subsystems: the internal system (system of interest), the boundary system (buffer system), and the external system (equivalent system), as illustrated by Figure 3.2, to facilitate analysis [19] [20].

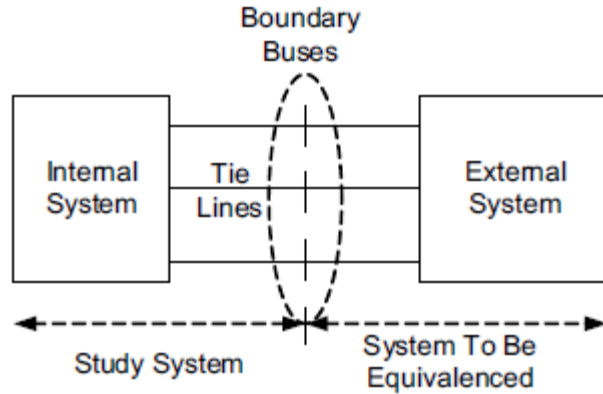


Figure 3.2 Partition of interconnected power system

The boundary system is selected so that the effects of disturbances in the external system upon the internal system are minimized. The boundary system can be properly established through offline contingency analysis or sensitivity analysis [21]. For example, long

transmission lines connecting two areas serve as good candidates for the boundary system. The external system can be approximated by modeling the remote boundary buses as PV buses, as illustrated in Figure 3.3, without sacrificing much accuracy.

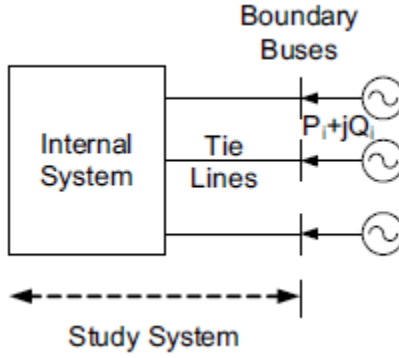


Figure 3.3 External system equivalent

The buses in the internal system can be classified into one of three categories: load bus, tie bus, and source bus. Load buses have load connected to them. A tie bus is a bus without load or any power generation device connected to it. Source buses include generator buses whose voltages are regulated by their connected generators, and boundary buses. A generator bus becomes a load bus if its connected generator reaches its capacity limit and loses its voltage regulation capability. Determination of whether a generator reaches its capacity limit can be achieved either by an indication signal from the generator over excitation limiter (OXL) or by detecting that the generator terminal voltage is below the regulated value for a defined period of time. A boundary bus becomes a load bus if the power flow direction switches from import to export.

Injection currents into the three types of buses can be expressed as:

$$\begin{bmatrix} i_L \\ i_T \\ i_G \end{bmatrix} = \begin{bmatrix} Y_{LL} & Y_{LT} & Y_{LG} \\ Y_{TL} & Y_{TT} & Y_{TG} \\ Y_{GL} & Y_{GT} & Y_{GG} \end{bmatrix} \begin{bmatrix} v_L \\ v_T \\ v_G \end{bmatrix} \quad (3.3)$$

where currents and voltages are complex numbers. The subscript L, T and G stand for load bus, tie bus and source bus respectively. The Y matrix is known as the system admittance that can be constructed from the network topology and network parameters.

From the equation 3.3, the load bus voltages can be expressed as a function of the injection currents to the load buses, the injection currents to the tie buses, the voltages of source buses, and the submatrices of the system admittance matrix.

$$v_L = Z_{LL}i_L + Z_{LT}i_T + H_{LG}v_G \quad (3.4)$$

where,

$$Z_{LL} = (Y_{LL} - Y_{LT}Y_{TT}^{-1}Y_{TL})^{-1} \quad (3.5)$$

$$Z_{LT} = -Z_{LL}Y_{LT}Y_{TT}^{-1} \quad (3.6)$$

$$H_{LG} = Z_{LL}(Y_{LT}Y_{TT}^{-1}Y_{TG} - Y_{LG}) \quad (3.7)$$

Because the injection currents to the tie buses are zero, the voltage of the j^{th} load bus can be expressed as

$$v_{Lj} = \sum_{i=1}^N Z_{LLji}i_{Li} + \sum_{k=1}^M H_{LGjk}v_{Gk} \quad (3.8)$$

where,

N is the number of load buses

M is the number of source buses.

Replacing the injection currents with the complex powers flowing out of the buses, the voltage of the j^{th} load bus can be expressed as

$$v_{Lj} = Z_{LLjj} \left(\frac{-S_{Lj}}{v_{Lj}} \right)^* + \sum_{i=1, i \neq j}^N Z_{LLji} \left(\frac{-S_{Li}}{v_{Li}} \right) + \sum_{k=1}^M H_{LGjk} v_{Gk} \quad (3.9)$$

Equation 3.9 can be rearranged into

$$\left(\frac{v_{equj} - v_{Lj}}{Z_{equj}} \right)^* v_{Lj} = S_{Lj} \quad (3.10)$$

where,

$$v_{equj} = \sum_{i=1, i \neq j}^N Z_{LLji} \left(\frac{-S_{Li}}{v_{Li}} \right)^* + \sum_{k=1}^M H_{LGjk} v_{Gk} \quad (3.11)$$

$$Z_{equj} = Z_{LLjj} \quad (3.12)$$

Equation 3.10 represents the power flow calculation of an equivalent simple system model as shown in figure 3.4.

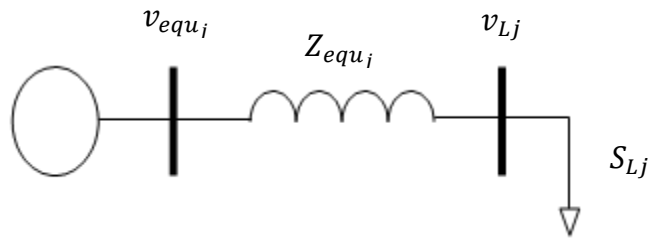


Figure 3.4 Simplified Thevenin Network

It is noted that the equivalent voltage source v_{equj} of the j^{th} load bus is a function of voltage sources and other system loads. The magnitude of the equivalent source voltage v_{equj} decreases as other system load demands increase. The equivalent impedance Z_{equj}

depends on the system topology, line characteristics, and bus type status. If there is no change in network topology and bus type, the equivalent impedance remains unchanged.

3.3 VSI BASED ON MAXIMUM POWER TRANSFERS

The Voltage Stability Index (VSI) [14] is based on the time synchronized measurements from the wide area monitoring systems. With time synchronized measurements of source voltage magnitude and power demand at the bus under study, the VSI is calculated by the minimum value between the ratios of three load margins. The VSI for a simple power system as shown in figure 3.5

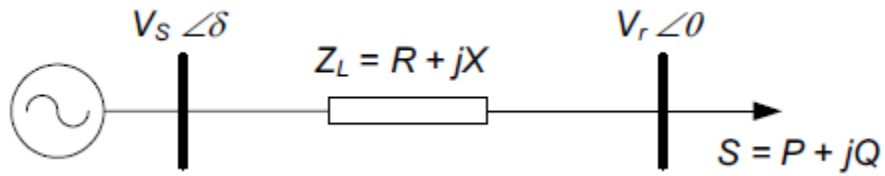


Figure 3.5 A simple power system to determine VSI

can be calculated using the equations 3.13-3.20

$$VSI = \min \left(\frac{P_{margin}}{P_{max}}, \frac{Q_{margin}}{Q_{max}}, \frac{S_{margin}}{S_{max}} \right) \quad (3.13)$$

where,

$$P_{margin} = P_{max} - P \quad (3.14)$$

$$Q_{margin} = Q_{max} - Q \quad (3.15)$$

$$S_{margin} = S_{max} - S \quad (3.16)$$

$$P_{max} = \sqrt{\frac{V_s^4}{4X^2} - \frac{QV_s^2}{X}} \quad (3.17)$$

$$Q_{max} = \frac{V_s^2}{4X} - \frac{P^2 X}{V_s^2} \quad (3.18)$$

$$S_{max} = \frac{(1 - \sin \theta) V_s^2}{2 \cos^2 \theta X} \quad (3.19)$$

$$\theta = \tan^{-1} \frac{Q}{P} \quad (3.20)$$

The VSI value varies from 0 to 1. If the value of the index is 1, it shows the system is stable and a value close to zero indicates unstable situation. If the value is 0, the voltage at a bus has collapsed.

3.4 VOLTAGE COLLAPSE PROXIMITY INDICATOR

Voltage stability evaluation using voltage at bus alone will not give a correct indication of an impending collapse. Voltage levels have to be studied as a function of some other key system parameter such as real power or reactive power. VOLTAGE COLLAPSE PROXIMITY INDICATOR (VCPI) [15] is derived from the basic power flow equation.

The technique is applicable for any number of buses in a system. It needs the voltage phasor information of the participating buses in the system and the network admittance matrix. VCPI uses the system admittance matrix instead of making a reduced equivalent system. A modified voltage phasor is first computed using the measurement value of voltage phasor at all buses along with admittance matrix.

For an N bus system the VCPI at bus k is given by,

$$VCPI_{k^{th} bus} = \left| 1 - \frac{\sum_{m=1, m \neq k}^N V'_m}{V_k} \right| \quad (3.21)$$

$$V'_m = \frac{Y_{km}}{\sum_{j=1, j \neq k}^N Y_{kj}} V_m = |V'_m| \angle \theta'_m \quad (3.22)$$

where,

V_k is the voltage phasor at bus k.

V_m is the voltage phasor at bus m.

Y_{km} is the admittance between buses k and m.

The VCPI is then computed which will vary from 0 to 1. If the index is 0, the bus is voltage stable and if the index is 1, the voltage at a bus has collapsed.

3.5 POWER TRANSFER STABILITY INDEX

Power Transfer Stability Index (PTSI) [16] as an index to measure voltage collapse using Thevenin equivalent of the system as shown in figure 3.6, where one of the buses is a slack bus connected to a load bus.

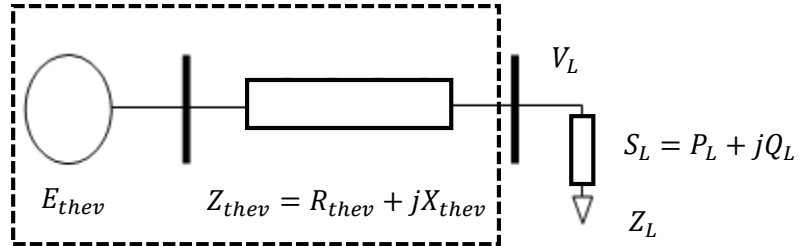


Figure 3.6 Simple two bus Thevenin equivalent system

The magnitude of load apparent power S_L can be expressed as

$$S_L = \frac{E_{thev}^2 Z_L}{Z_{thev}^2 + Z_L^2 + 2Z_{thev}Z_L \cos(\beta - \alpha)} \quad (3.23)$$

where, α is phase angle of the load impedance and β is phase angle of the Thevenin impedance.

The maximum load apparent power S_{Lmax} is given by

$$S_{Lmax} = \frac{E_{thev}^2}{2Z_{thev}(1+\cos(\beta-\alpha))} \quad (3.24)$$

The maximum load apparent power is also considered as a maximum loadability limit which depends on the Thevenin parameters that vary with system operating conditions.

To assess the load bus distance to voltage collapse, a power margin is defined as $S_{Lmax} - S_L$ in which the margin is equal to 0 if $Z_L = Z_{thev}$. For power margin values equal to 0, it indicates that no more power can be transferred at this point and a proximity to voltage collapse is said to occur. Thus, to prevent a power system from voltage collapse, the power margin has to be greater than 0. In other words, the ratio of S_L to S_{Lmax} has to be less than 1. However a voltage collapse will occur if the ratio of S_L to S_{Lmax} is equal to 1.

Power Transfer stability index is defined as

$$PTSI = \frac{S_L}{S_{Lmax}} \quad (3.25)$$

$$PTSI = \frac{2S_L Z_{thev}(1+\cos(\beta-\alpha))}{E_{thev}^2} \quad (3.26)$$

The value of PTSI will fall between 0 and 1. When PTSI value reaches 1, it indicates that voltage collapse has occurred.

CHAPTER 4

TEST SYSTEM AND TEST CASES

Digsilent PowerFactory software is used for this work. All the load flow analysis and steady state analysis are done in Power Factory. Three indices taken for the study VSI, VCPI and PTSI are implemented using Matlab. Voltage stability analysis is done on IEEE 14 Bus system. This chapter will give a brief introduction to Digsilent PowerFactory and a detailed description of IEEE 14 Bus system. The test cases for voltage instability analysis is also explained.

4.1 DIGSILENT POWERFACTORY

Digsilent PowerFactory is a leading power system analysis software for applications in generation, transmission, distribution and industrial systems. It is integrating all required functions, easy to use, fully Windows compatible and combines reliable and flexible system modelling capabilities with state-of-the-art algorithms and a unique database concept. It is easy to use and caters for all standard power system analysis needs, including high-end applications in new technologies such as wind power and distributed generation and the handling of very large power systems. In addition to the stand-alone solution, the PowerFactory engine can be smoothly integrated into GIS, DMS and EMS supporting open system standards.

PowerFactory has two types of functions, basic and advanced. Basic functions include Load Flow Analysis, Short-Circuit Analysis, Load Flow Sensitivities, Asynchronous Machine Parameter Identification, Overhead Line and Cable Parameter Calculation and Basic MV/LV Network Analysis. Advanced functions include Contingency Analysis,

Quasi-Dynamic Simulation, Network Reduction Protection Functions, Arc-Flash Hazard Analysis, Cable Analysis, Power Quality and Harmonic Analysis, Connection Request Assessment, Transmission Network Tools, Distribution Network Tools, Reliability Analysis, Optimal Power Flow (OPF), Techno-Economical Analysis, State Estimation, Stability Analysis Functions (RMS), Electromagnetic Transients (EMT), Motor Starting Functions, Small Signal Stability, System Parameter Identification and Scripting and Automation.

For this study, the following load flow assumptions are made: The system frequency is uniform at 50Hz with a 100MVA base. All buses contain PMUs, therefore the entire system is observable and can output measurements as described in previous chapters. All generator AVR's regulate at scheduled voltage for all generator bus until the MVAR capability limit has been reached. Loads are constant power loads, unless mentioned otherwise. Transmission lines are based on the equivalent Pi-model containing an equivalent resistance, reactance, and shunt impedance. All lines will assume infinite ampacity, however, ratings will be used for analysis purposes only. Lastly, the voltage collapse point is assumed to be when the power flow does not converge to a solution.

4.2 IEEE 14 BUS SYSTEM

The 14 Bus System consists of 14 buses, 5 generators, 11 loads, 16 lines, 5 transformers. 3 of these 5 transformers are used to represent one single 3-winding transformer. Figure 4.1 shows the single line diagram. It is a simplified model of the transmission system in the Midwest United States.

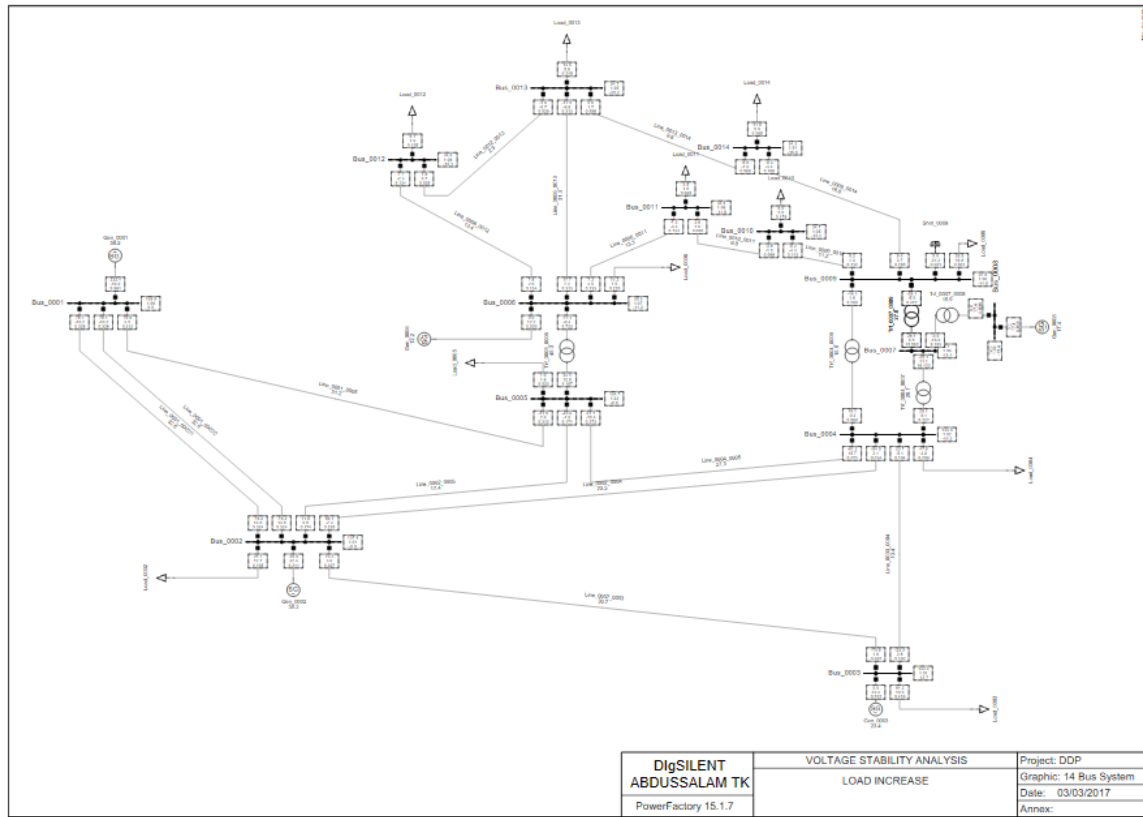


Figure 4.1 IEEE 14 Bus Test System

The system base case conditions are given in per unit values, unless specified otherwise and are shown in tables 4.1, 4.2 and 4.3.

Bus Number	Bus Type	Voltage (pu)	Pgen (MW)	Qgen (MVAR)	Pmax (MW)	Qmin (MVAR)	Qmax (MVAR)
1	Slack	1.060	232.29	-16.89	300	-70	80
2	PV	1.045	40.00	42.40	80	-40	50
3	PV	1.010	0.00	23.39	80	0	40
6	PV	1.070	0.00	12.24	80	-6	24
8	PV	1.090	0.00	17.36	80	-6	24

Table 4.1 IEEE 14 Bus System- Generator Data

Bus Number	Voltage (pu)	Pload (MW)	Qload(MVAR)
2	1.045	21.7	12.7
3	1.010	94.2	19
4	1.019	47.8	-3.9
5	1.020	7.6	1.6
6	1.070	11.2	7.5
9	1.056	29.5	16.6
10	1.051	9	5.8
11	1.057	3.5	1.8
12	1.055	6.1	1.6
13	1.050	13.5	5.8
14	1.036	14.9	5

Table 4.2 IEEE 14 Bus System- Load Data

From Bus	To Bus	R(pu)	X(pu)	B(pu)
1	2	0.01938	0.05917	0.0528
1	5	0.05403	0.22304	0.0492
2	3	0.04699	0.19797	0.0438
2	4	0.05811	0.17632	0.0374
2	5	0.05695	0.17388	0.034
3	4	0.06701	0.17103	0.0346
4	5	0.01335	0.04211	0.0128
6	11	0.09498	0.19890	0.0000
6	12	0.12291	0.25581	0.0000
6	13	0.06615	0.13027	0.0000
9	10	0.03181	0.08450	0.0000
9	14	0.12711	0.27038	0.0000
10	11	0.08205	0.19207	0.0000
12	13	0.22092	0.19988	0.0000
13	14	0.17093	0.34802	0.0000

Table 4.3 IEEE 14 Bus System- Line Data

4.3 TEST CASES

For analysing the indices, different test cases need to be developed. These test cases should reflect possible real life situations. Three test cases are considered and the simulation of these cases are done using PowerFactory. This section will discuss about the test cases.

4.3.1 Increasing Load Demand

One of the main problems in power system is the instability occurred because of the high load demand, which happens when system generation can no longer supply the demand. This condition often takes place when the load demand is under predicted. Due to the complex nature of loads, the representation of this situation can be carried out in many ways. For this study, the selected loads will be increased at constant power factor until the system collapses.

4.3.2 Increasing Load Reactive Power Demand

Reactive power is closely linked to voltage, it is observed from the QV curve. As the reactive power demand increases the system losses increase, this will result in various instability issues. For this study, only reactive power at the selected loads will be increased until the system collapses.

4.3.3 Line Outage

During high demand times, the power supply through lines increase. When the power flow through the line reaches the line limit, outage of line may happen. So, it is useful to consider contingencies like line outage for voltage stability analysis.

4.4 SYNOPSIS OF INDICES

Publication	Index	Stable Condition	Unstable Condition
[27]	VSI_k $= \min \left(\frac{P_{margin}}{P_{max}}, \frac{Q_{margin}}{Q_{max}}, \frac{S_{margin}}{S_{max}} \right)$	$VSI \rightarrow 1$	$VSI \rightarrow 0$
[31]	$VCPI_{k^{th} bus} = \left 1 - \frac{\sum_{m=1, m \neq k}^N V'_m}{V_k} \right $	$VCPI \rightarrow 0$	$VCPI \rightarrow 1$
[32]	$PTSI_k = \frac{2S_L Z_{thev} (1 + \cos(\beta - \alpha))}{E_{thev}^2}$	$PTSI \rightarrow 0$	$PTSI \rightarrow 1$

Table 4.4 Summary of Selected Indices

The algorithms for obtaining VCPI, VSI and PTSI are shown in figures 4.2, 4.3 and 4.4 respectively.

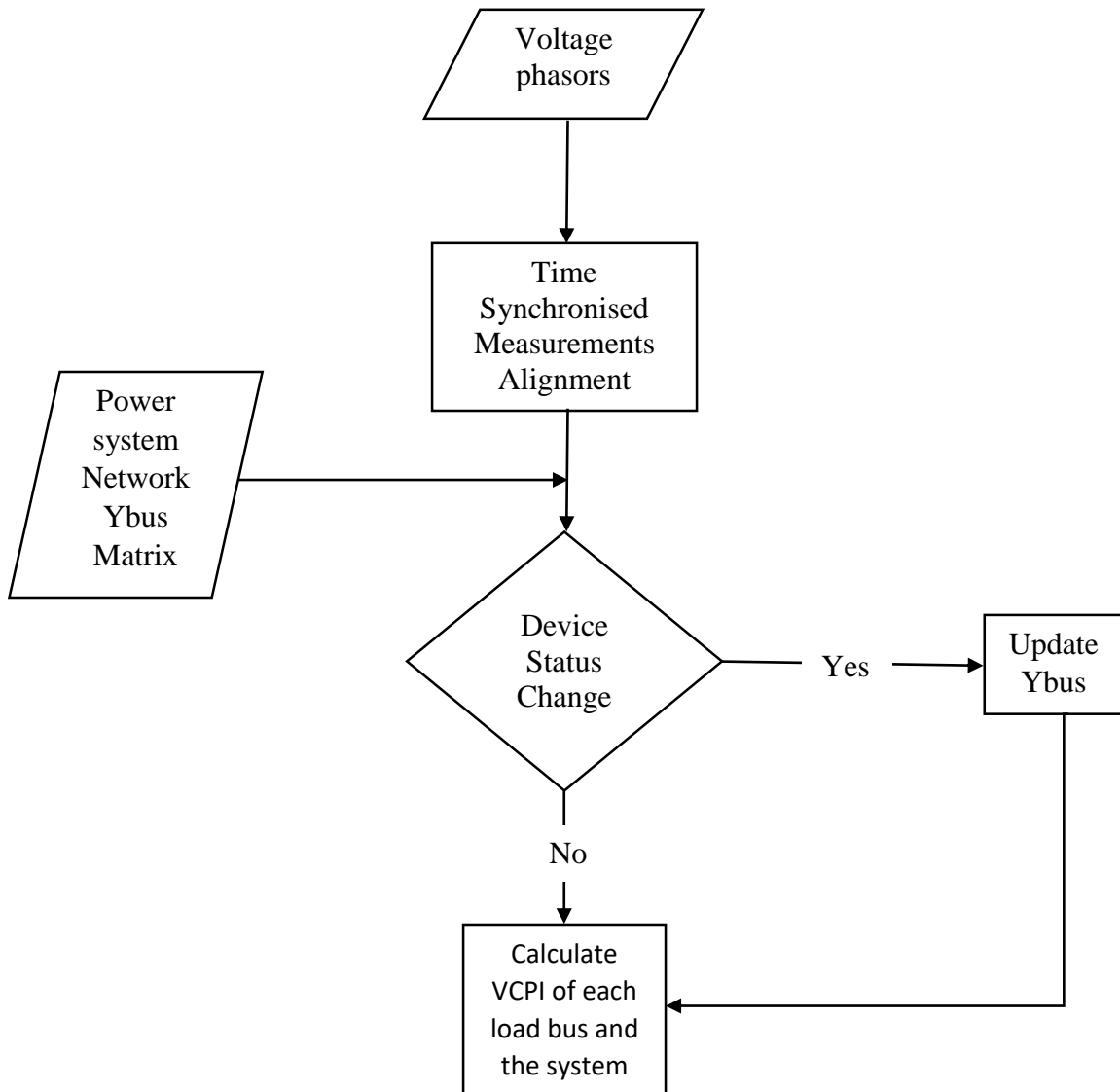


Figure 4.2 Algorithm for Computing VCPI

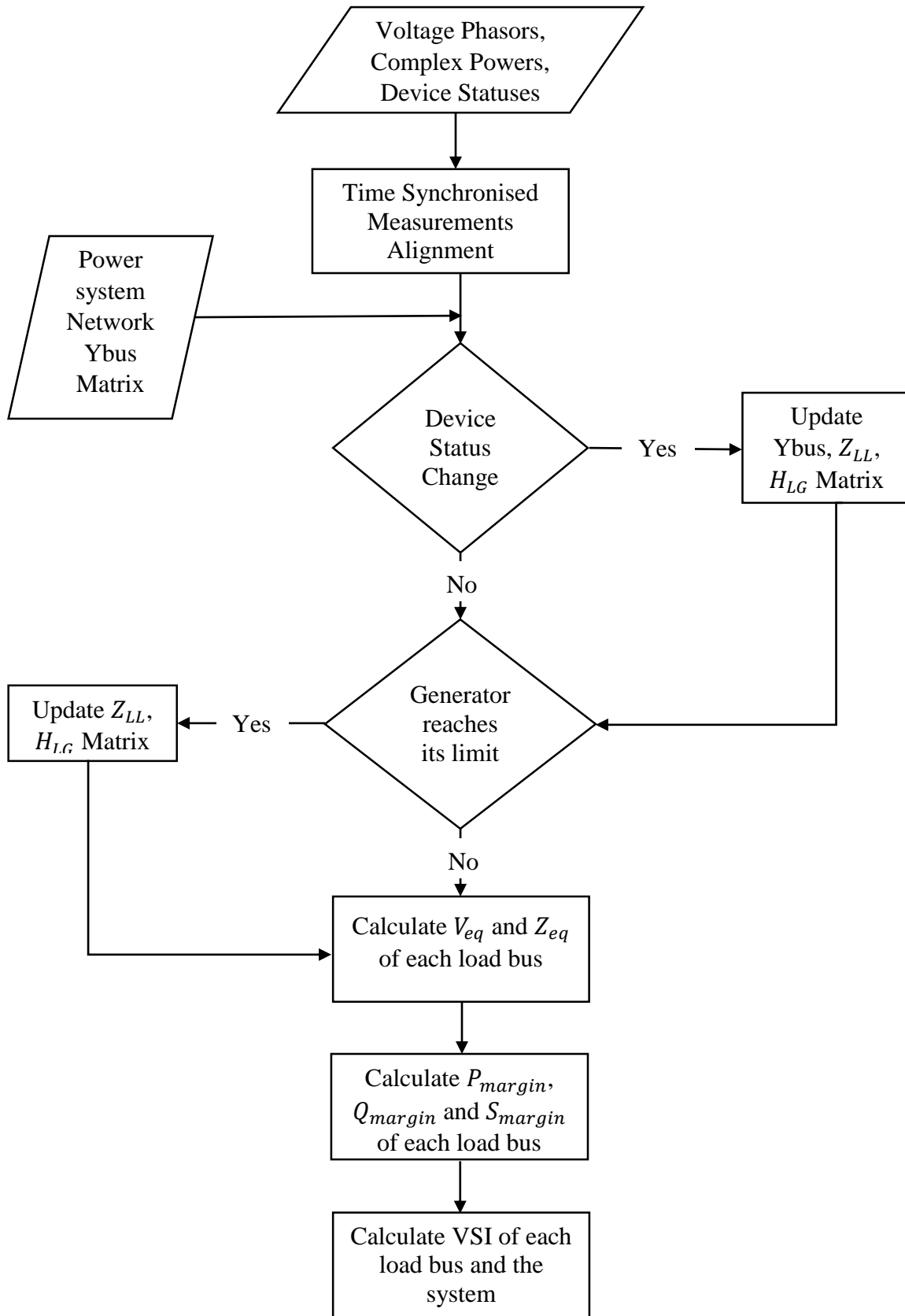


Figure 4.3 Algorithm for Computing VSI

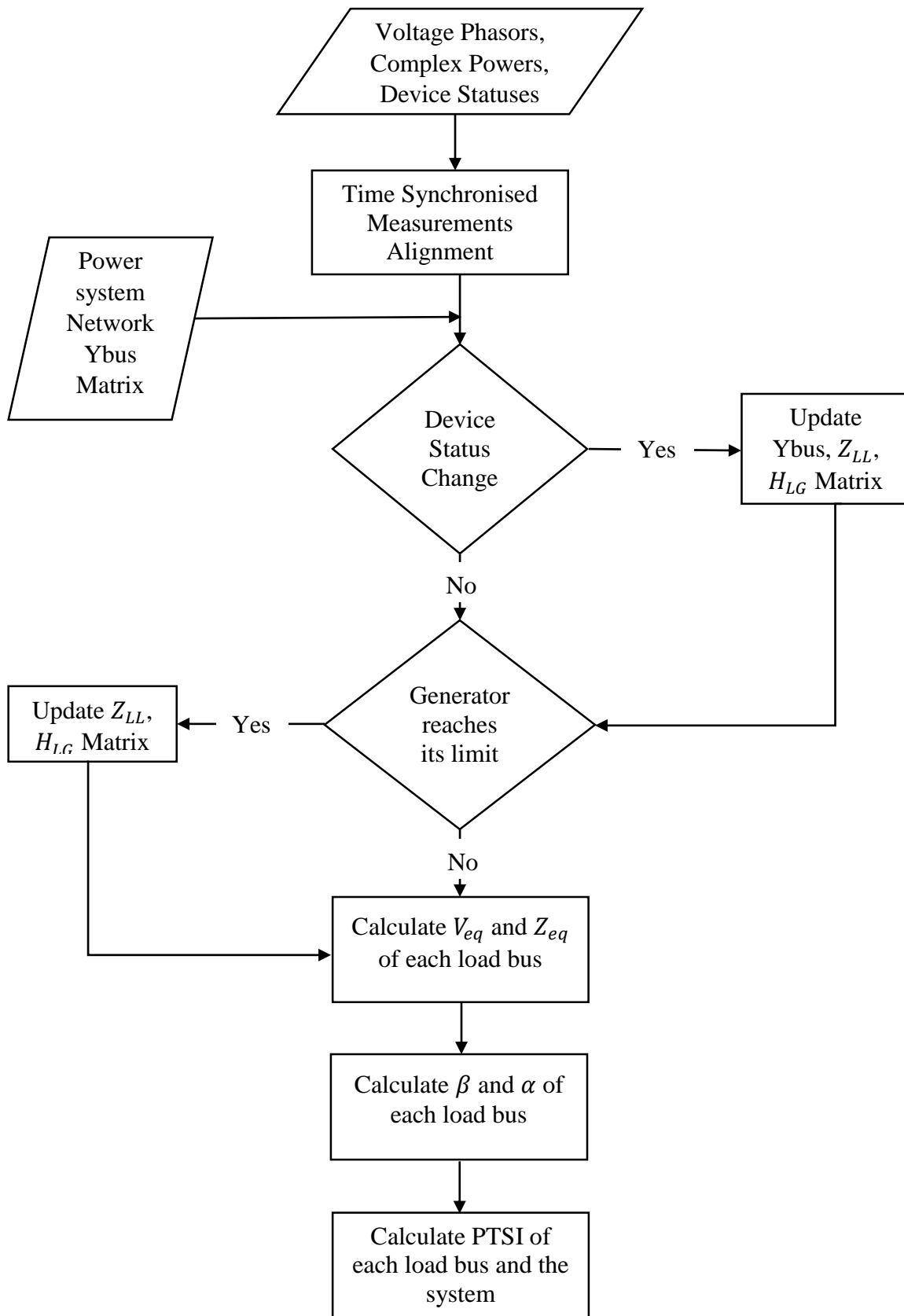


Figure 4.4 Algorithm for Computing PTSI

CHAPTER 5

SIMULATION RESULTS

Three test cases are taken for voltage stability analysis. The simulation of IEEE 14 bus system is done using PowerFactory. To find the values of the indices, a series of load flow analysis were conducted on Power factory. The PMU inputs: voltage magnitude, voltage angle, load powers and admittance matrix after each change were outputted to Matlab. Results of the indices are discussed in this section for each test cases.

5.1 CASE 1: INCREASING LOAD DEMAND

The loads in the 14 bus system were subjected to real power increase at constant power factor. Each load was increased by 10% of the base case until the system collapsed, which is observed when the load was increased by 1.65 times the base case. Table 5.1 shows the total load for each case.

Load Factor	Base Case	1.1	1.2	1.3	1.4	1.5	1.6
Load Demand	259	284.9	310.8	336.7	362.6	388.5	414.4

Table 5.1 Load factor with corresponding Total System Load

The system is operating under the base case condition initially. When the load demand increased to 1.2 times the base case, generator at bus 3 reaches its reactive limit. When the load demand increased to 1.4 times the base case, generators at buses 6 and 8 reach their

reactive limit. Upon the next load increase, 1.5 times the base case, generator at bus 2 reaches its reactive limit. When the load demand is increased to 1.65, the system could not maintain its stability, resulted in a system collapse. The VSI, VCPI and PTSI for each load increase are shown in tables 5.2, 5.3 and 5.4 respectively.

Factor Bus	1	1.1	1.2	1.3	1.4	1.5	1.6
4	0.958	0.953	0.945	0.937	0.923	0.907	0.852
5	0.934	0.929	0.924	0.917	0.910	0.902	0.889
9	0.853	0.843	0.832	0.817	0.596	0.281	0.099
10	0.877	0.843	0.801	0.758	0.672	0.591	0.134
11	0.915	0.910	0.904	0.888	0.877	0.766	0.405
12	0.916	0.913	0.909	0.906	0.901	0.836	0.468
13	0.929	0.925	0.920	0.915	0.903	0.843	0.527
14	0.915	0.911	0.872	0.861	0.786	0.738	0.274

Table 5.2 VSI for different Load Factors (CASE 1)

Factor Bus	1	1.1	1.2	1.3	1.4	1.5	1.6
4	0.152	0.177	0.193	0.217	0.243	0.307	0.352
5	0.209	0.216	0.223	0.231	0.239	0.248	0.261
9	0.671	0.696	0.722	0.749	0.779	0.822	0.953
10	0.277	0.293	0.313	0.335	0.366	0.399	0.539
11	0.175	0.186	0.197	0.209	0.212	0.229	0.305
12	0.139	0.144	0.150	0.157	0.165	0.175	0.201
13	0.149	0.158	0.167	0.176	0.188	0.203	0.244
14	0.102	0.109	0.116	0.122	0.128	0.138	0.174

Table 5.3 VCPI for different Load factors (CASE 1)

Factor Bus	1	1.1	1.2	1.3	1.4	1.5	1.6
4	0.104	0.111	0.125	0.168	0.216	0.279	0.332
5	0.115	0.121	0.139	0.159	0.201	0.254	0.312
9	0.261	0.269	0.306	0.389	0.588	0.762	0.926
10	0.189	0.211	0.281	0.366	0.561	0.730	0.894
11	0.101	0.124	0.170	0.214	0.273	0.371	0.516
12	0.085	0.221	0.328	0.425	0.490	0.557	0.654
13	0.066	0.101	0.116	0.151	0.199	0.230	0.408
14	0.105	0.199	0.231	0.250	0.278	0.329	0.707

Table 5.4 PTSI for different load factors (CASE 1)

The VSIs, VCPIs and PTSIs that showed values near to unstable condition before collapsing are plotted to illustrate an overall pattern on figures 5.1, 5.2 and 5.3 respectively.

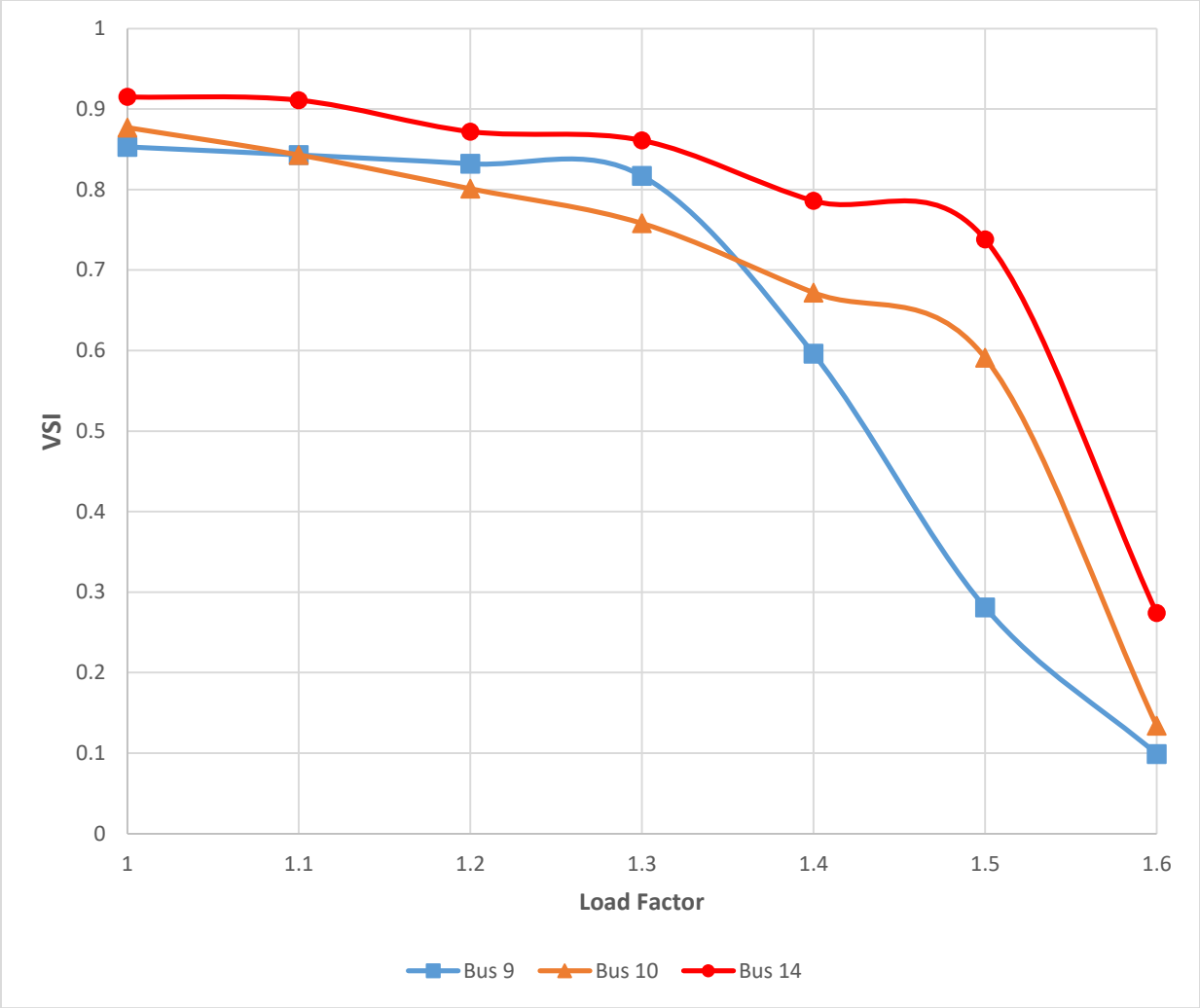


Figure 5.1 VSI for Load Buses 9, 10 and 14 (CASE 1)

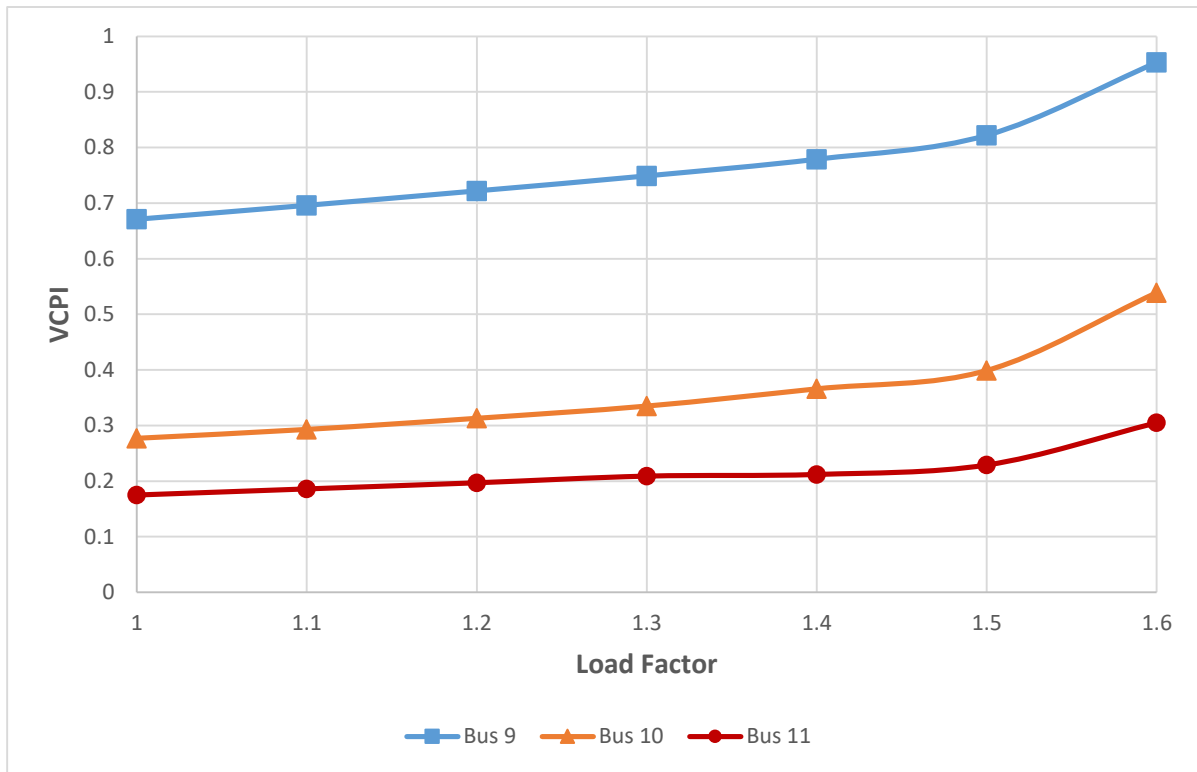


Figure 5.2 VCPI for Load Buses 9, 10 and 11 (CASE 1)

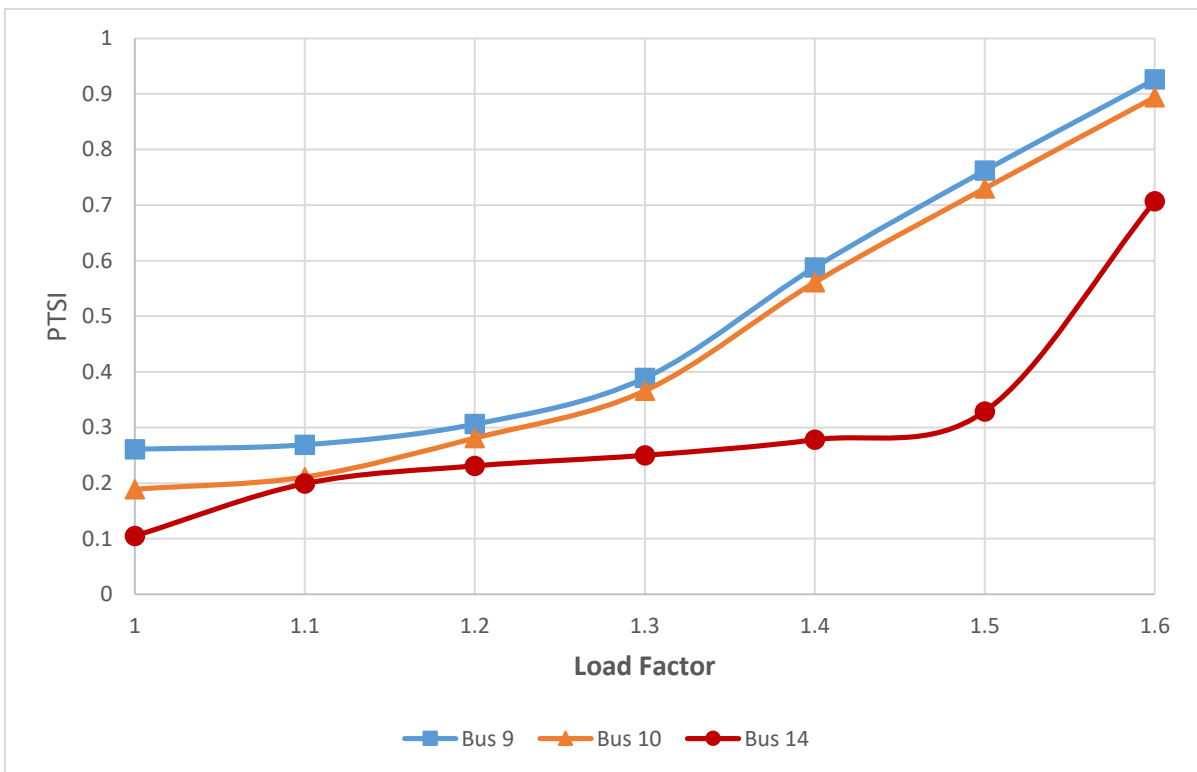


Figure 5.3 PTSI for Buses 9, 10 and 14 (CASE 1)

5.2 CASE 2: INCREASING LOAD REACTIVE POWER DEMAND

The loads in the 14 Bus system were subjected to reactive power increase. Each load was increased by 10 % of the base case until the system collapsed. At 1.4 times the base case, generator at bus 3 reaches its reactive limit. When the demand was increased to 1.8 times, generators at buses 6 and 8 reach their limit. Generator at bus 2 reaches its reactive limit when demand was increased to 1.9 times the base case. The system collapses when the total reactive load was increased to 2 times the base case. The indices are tabulated in the tables 5.5, 5.6 and 5.7.

Factor \ Bus	1	1.1	1.2	1.3	1.4	1.5	1.6	1.7	1.8	1.9	2.0
4	0.958	0.942	0.941	0.940	0.938	0.936	0.933	0.929	0.922	0.916	0.856
5	0.934	0.934	0.930	0.926	0.922	0.916	0.914	0.912	0.910	0.908	0.906
9	0.853	0.852	0.851	0.849	0.814	0.728	0.639	0.462	0.361	0.221	0.096
10	0.877	0.850	0.815	0.809	0.801	0.791	0.742	0.658	0.561	0.512	0.156
11	0.915	0.900	0.890	0.855	0.879	0.863	0.831	0.775	0.591	0.546	0.279
12	0.916	0.914	0.911	0.910	0.905	0.898	0.879	0.866	0.624	0.564	0.355
13	0.929	0.916	0.915	0.913	0.911	0.901	0.875	0.861	0.762	0.759	0.623
14	0.915	0.914	0.913	0.903	0.901	0.896	0.879	0.811	0.721	0.658	0.459

Table 5.5 VSI for CASE 2

Factor Bus	1	1.1	1.2	1.3	1.4	1.5	1.6	1.7	1.8	1.9	2.0
4	0.152	0.153	0.152	0.154	0.154	0.156	0.158	0.159	0.157	0.158	0.156
5	0.209	0.211	0.211	0.215	0.214	0.213	0.210	0.219	0.218	0.210	0.209
9	0.671	0.671	0.675	0.683	0.742	0.809	0.858	0.892	0.956	0.969	1.001
10	0.277	0.281	0.287	0.291	0.296	0.301	0.309	0.315	0.319	0.327	0.348
11	0.175	0.178	0.181	0.184	0.189	0.191	0.194	0.203	0.211	0.230	0.266
12	0.139	0.141	0.143	0.144	0.145	0.146	0.147	0.151	0.168	0.189	0.201
13	0.149	0.151	0.153	0.155	0.158	0.159	0.161	0.165	0.169	0.182	0.199
14	0.102	0.102	0.103	0.105	0.107	0.109	0.113	0.115	0.118	0.121	0.123

Table 5.6 VCPI for Case 2

Factor Bus	1	1.1	1.2	1.3	1.4	1.5	1.6	1.7	1.8	1.9	2.0
4	0.104	0.112	0.131	0.140	0.158	0.176	0.193	0.209	0.222	0.236	0.257
5	0.115	0.124	0.130	0.136	0.142	0.151	0.162	0.172	0.183	0.198	0.216
9	0.261	0.263	0.271	0.329	0.354	0.428	0.459	0.482	0.541	0.721	0.908
10	0.189	0.191	0.205	0.209	0.301	0.391	0.441	0.559	0.663	0.712	0.856
11	0.101	0.110	0.121	0.156	0.176	0.264	0.331	0.476	0.596	0.649	0.828
12	0.085	0.103	0.112	0.131	0.141	0.278	0.351	0.372	0.464	0.581	0.655
13	0.066	0.086	0.099	0.115	0.145	0.173	0.186	0.272	0.332	0.361	0.422
14	0.105	0.119	0.127	0.139	0.168	0.191	0.214	0.241	0.332	0.446	0.521

Table 5.7 PTSI for Case 2

The indices values for the buses which are close to unstable conditions are plotted in figures 5.4, 5.5 and 5.6.

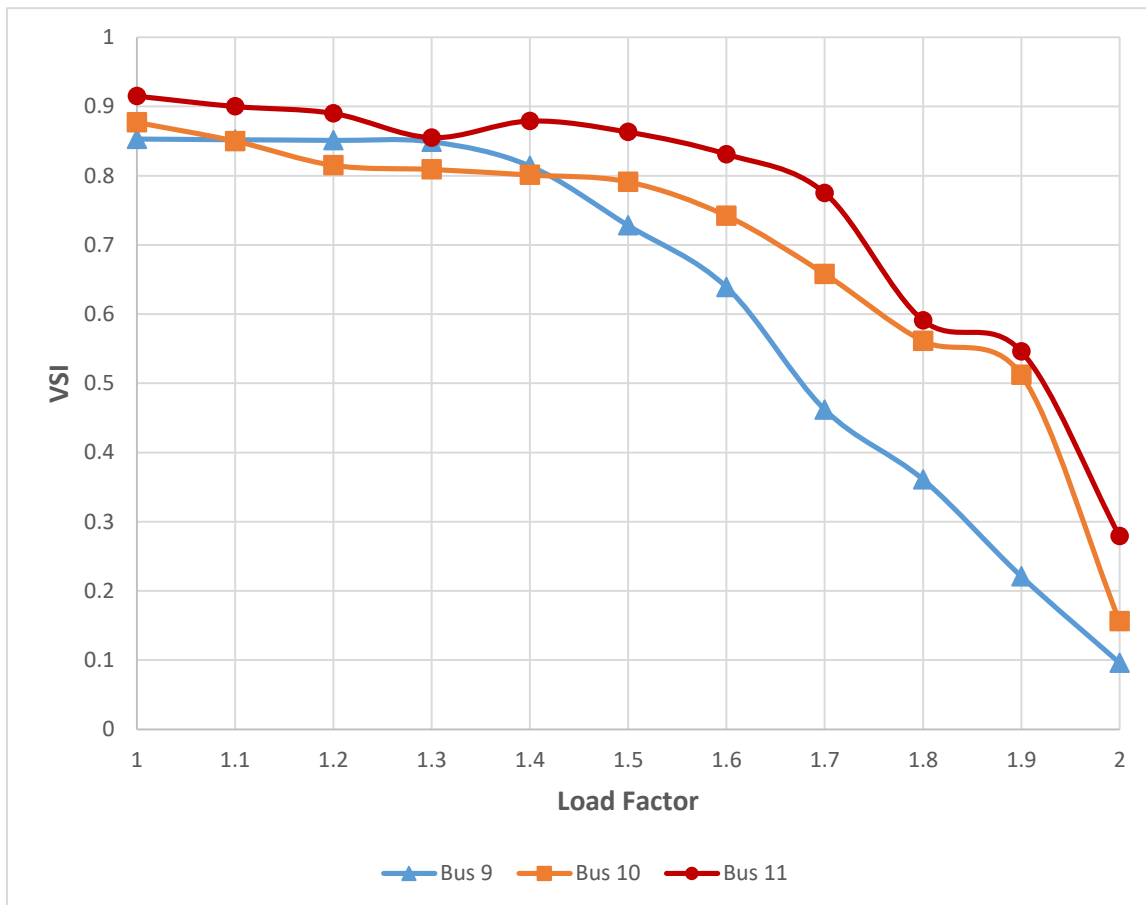


Figure 5.4 VSI for Case 2: Bus 9, 10 and 11

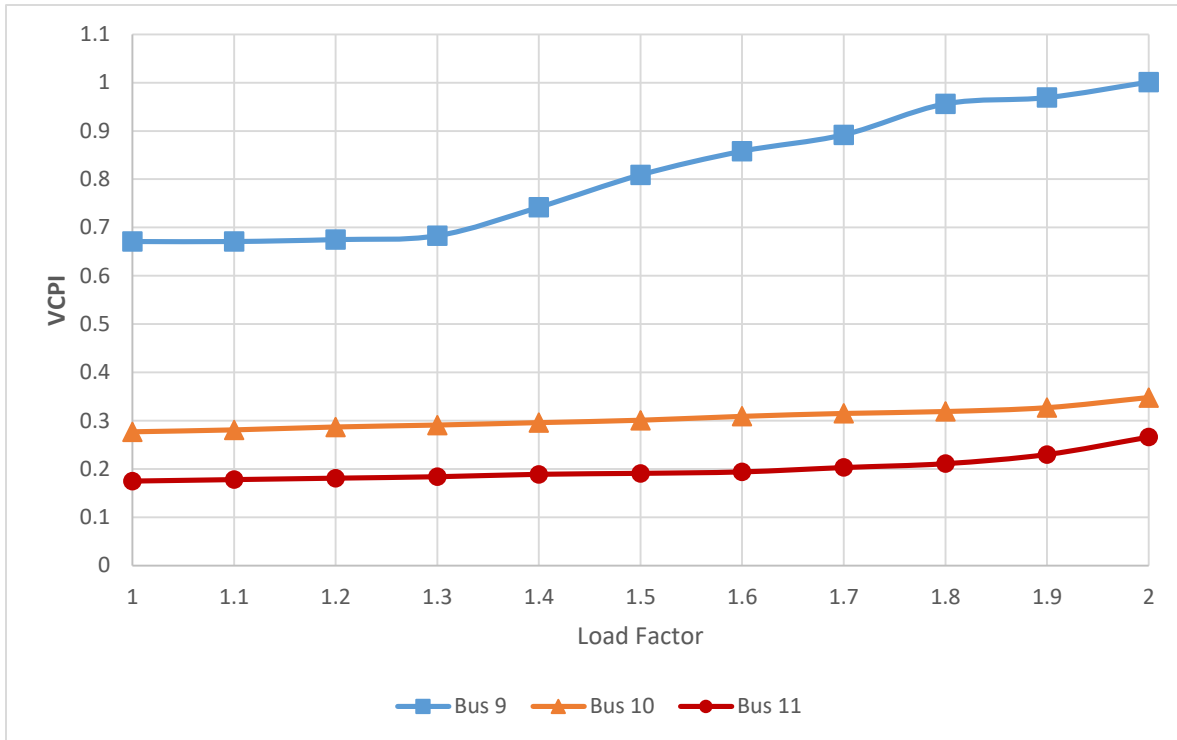


Figure 5.5 VCPI for Case 2: Bus 9, 10 and 11

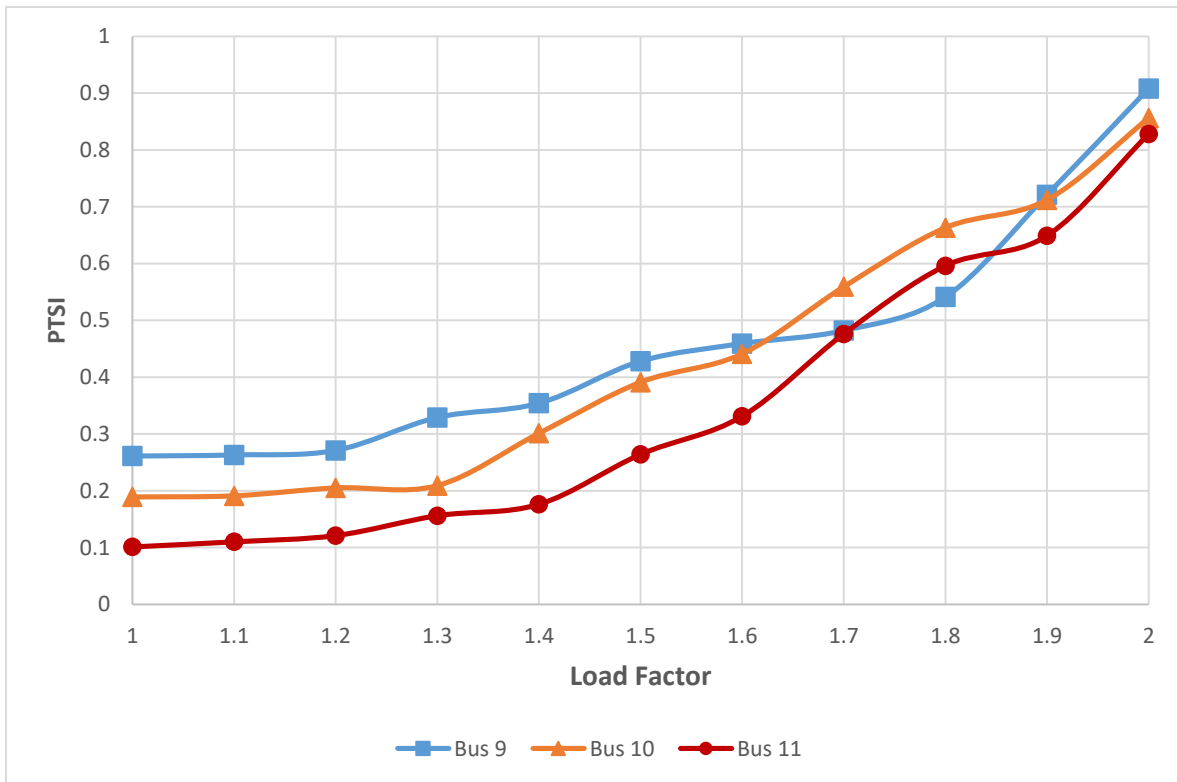


Figure 5.6 PTSI for Case 2: Bus 9, 10 and 11

5.3 LINE OUTAGE

As in the first case, the loads in the 14 bus system were subjected real power increase at constant power factor. Each load was increased by 5%. When the load demand was increased to 1.4 times the base case, a transmission line was disconnected to simulate the loss of a heavily loaded line. The line was chosen based on the limit of the line, the line which has reached near its maximum capacity was disconnected. For this study line 1-5 is disconnected.

Bus	VSI			VCPI			PTSI		
	Before	After	%Δ	Before	After	%Δ	Before	After	%Δ
4	0.923	0.920	-0.325	0.243	0.250	2.881	0.216	0.218	0.926
5	0.910	0.895	-1.648	0.239	0.255	6.694	0.201	0.210	4.478
9	0.596	0.594	-0.336	0.779	0.781	0.257	0.588	0.591	0.510
10	0.672	0.671	-0.149	0.366	0.368	0.546	0.561	0.564	0.535
11	0.877	0.851	-2.965	0.212	0.215	1.415	0.273	0.281	2.930
12	0.901	0.886	-1.665	0.165	0.168	1.818	0.490	0.497	1.428
13	0.903	0.889	-1.550	0.188	0.190	1.064	0.199	0.204	2.512
14	0.786	0.785	-0.127	0.128	0.129	0.781	0.278	0.280	0.719

Table 5.8 Values of Indices Before And After Line tripped

From table 5.8, all the three indices show that the removal of the line has great impact on buses 5, 11, 12 and 13. VSI shows the most significant change on bus 11, while VCPI and PTSI show the most significant change on bus 5. The affected buses are close to the removed line.

5.4 VOLTAGE COLLAPSE PREDICTABILITY FROM INDICES

Voltage stability indices should be able to represent the state of the system and results can be understood at an intuitive level. So, it is important it is important to find whether an

index can detect the proximity to voltage collapse without knowing the nature of the load. To determine this, the values of the indices just before the system collapse for case 1 and case 2 are considered.

Factor Bus	VSI		VCPI		PTSI	
	Case 1	Case 2	Case 1	Case 2	Case 1	Case 2
	1.6	2	1.6	2	1.6	2
4	0.852	0.856	0.352	0.156	0.332	0.257
5	0.889	0.906	0.261	0.209	0.312	0.216
9	0.099	0.096	0.953	1.001	0.926	0.908
10	0.134	0.156	0.539	0.348	0.894	0.856
11	0.405	0.279	0.305	0.266	0.516	0.828
12	0.468	0.355	0.201	0.201	0.654	0.655
13	0.527	0.623	0.244	0.199	0.408	0.422
14	0.274	0.459	0.174	0.123	0.707	0.521

Table 5.9 Indices before collapse: Case 1 and Case 2

By comparing the values of indices before collapse, it is clear that most of the indices approach similar values, showing that the indices are independent of the nature the load near voltage collapse. Buses that show a difference of .15 between the cases are highlighted.

5.5 WEAKEST BUS

The indices can be used to determine the strength of each bus depending on the value of each index. The indices used for analysis in this thesis do not present any method to determine the weak determine the weak buses. An attempt to determine the weakest bus is done by considering the indices values for first load increase and indices values before collapse in case 1.

Table 5.10 and 5.11 show the rankings of first load increase and last load increase for the three indices respectively.

	VSI		VCPI		PTSI	
Ranking	Bus	Index	Bus	Index	Bus	Index
1	9	0.843	9	0.696	9	0.269
2	10	0.843	10	0.293	12	0.221
3	11	0.91	5	0.216	10	0.211
4	14	0.911	11	0.186	14	0.199
5	12	0.913	4	0.177	11	0.124
6	13	0.925	13	0.158	5	0.121
7	5	0.929	12	0.144	4	0.111
8	4	0.953	14	0.109	13	0.101

Table 5.10 Comparison of Rankings between the Indices: First Load Increase

All the three indices for first load increase show that Bus 9 is the weakest. But, it is not possible to conclude that with without considering the final load increase. Bus 2 is ranked by VSI and VCPI values but PTSI values show it as 3 in rankings. So, these information are insufficient to make any conclusion. Now, consider the case of last load increase before system collapse.

	VSI		VCPI		PTSI	
Ranking	Bus	Index	Bus	Index	Bus	Index
1	9	0.099	9	0.953	9	0.926
2	10	0.134	10	0.539	10	0.894
3	14	0.274	4	0.352	14	0.707
4	11	0.405	11	0.305	12	0.654
5	12	0.468	5	0.261	11	0.516
6	13	0.527	13	0.244	13	0.408
7	4	0.852	12	0.201	4	0.332
8	5	0.889	14	0.174	5	0.312

Table 5.11 Comparison of Rankings between the Indices: Final Load Increase

In this case, all the three indices show that bus 9 is the weakest bus. From these two cases we can say that bus 9 is the weakest or critical one. There may be some chances that this is not true because these indices consider apparent power, real power, reactive power and admittances only. There are some other factors that can make instability in the system. These can be seen from the Rankings of other buses, Rankings are not matching. So, additional studies should be done in order to establish an appropriate relationship between instability and various quantities.

5.6 STABILITY MARGIN

The indices were able to detect the instability limits in 14 bus system. Indices approach their instability condition values when the system is on the verge of collapse. From indices values, to determine the state of the system, a margin should be made which distinguishes when the system is near a collapse. By considering the critical index values before collapse for case 1 and case 2, VSI provides an index of 0.281 and 0.221. Similarly, VCPI provides an index of 0.822 and 0.969 respectively, PTSI provides an index of 0.762 and 0.721 respectively. Considering the fact that a system collapse can occur within seconds, the margin should be established to give sufficient time to study and respond to the situation. For the three indices, a 0.3 index margin should be appropriate.

CHAPTER 6

CONCLUSION AND FUTURE SCOPE

Voltage stability analysis using simulated synchrophasor data was done in thesis. Three indices from literature, VSI, VCPI and PTSI were examined in order to show how the PMU data can be used to determine how far the system is from its voltage collapse point. Steady state analysis for the test cases was performed using DigSilent Powerfactory software, and the indices were implemented using Matlab. Three test cases were considered for the analysis, increasing real power load demand at constant power factor, increasing reactive power demand and Line outage. The performances of the indices were tested in IEEE 14 Bus system. For a stable system, values of the indices fall between 0 and 1. From the results, it is observed that VCPI can exceed 1 when the system is unstable.

While comparing the three indices, VSI and PTSI provide a more intuitive index compared to VCPI for predicting the instability. VCPI does not give any predictable value for almost all buses at the voltage stability boundary. VCPI cannot estimate the voltage stability margin but they can be used to determine critical lines or buses for a given load level. VCPI calculation is very fast and easy when comparing with PTSI and VSI. A stability margin of 0.3 should be used for the indices, which can allow the system operator to initiate the remedial actions necessary to prevent voltage collapse.

Voltage collapse can be predicted from the index, and regardless of load type the index will still approach the same value. The curve shows a nonlinear trend near the voltage collapse point. Each index changes automatically with different operating conditions and does not depend on any particular scenario. Low voltage and reactive margin do not necessarily

indicate a critical bus. Additional parameters such as powers, system topology should be considered when making such an analysis.

One of the main objectives of this thesis was investigate if the state of the system could be determined by looking at only the index values. Therefore a majority of the plots presented only show the index values per a given variable. It may be useful to plot voltage values alongside with the indices in order to define other relationships between indices and voltage.

Since this thesis analysed these three indices using a steady state analysis approach, a natural extension to this is to conduct similar studies using a time-based dynamic analysis approach. This requires an accurate model of the system that represents the transients associated with a voltage collapse. A dynamic simulation can demonstrate the time response of the system voltage with respect to a series of events. Therefore, helping to identify whether the system voltage is stable or not. Using this approach, an analysis can reveal the actual mechanisms of voltage instability and how the indices respond to it.

APPENDIX A

Matlab Code

```
%this code computes VSI of 14 bus system
%case: increasing load demand at constant power factor
%m-file input: thevequiv.m

compVSI = 0;
for j=1:7 %j is the load factor sequence in the case
[Vx,Z,Spower,Y] = thevequiv(j);
Ybus=Y;
for i =1:8
R=real(Z(i));
X=imag(Z(i));
S = abs(Spower(i));
P = real(Spower(i));
Q = imag(Spower(i));
Vs = abs(Vx(i));
theta = atan(Q/P); %in radians
Pmax = (Q*R/X) - ((Vs^2)*R)/(2*X^2) + abs(Z(i))*Vs*sqrt((Vs^2) - 4*Q*X)/(2*X^2);
Qmax = ((Vs^2)/(4*X) - (P^2)*X/(Vs^2));
Smax = (Vs^2)*(abs(Z(i)) - (sin(theta)*X+cos(theta)*R))/(2*(cos(theta)*Xsin(theta)*R)^2);
%calculate Margins
Smargin = Smax - S;
Pmargin = Pmax - P;
Qmargin = Qmax - Q;
%compute individual VSI
VSI=[Pmargin/Pmax, Qmargin/Qmax, Smargin/Smax];
%load bus VSI
compVSI(i,j)=min(VSI);
end
end

%*****

%this code computes VSI of 14 bus system
%case: increasing load demand at constant power factor
%m-file input: thevequiv.m,synchrophasor.m

compPTSI = 0;
for j=1:7 %j is the load factor sequence in the case
[Vx,Z,Spower,Y] = thevequiv(j);
[V,S,gens,ybus] = synchrophasor(j);
```



```

for i =1:8
beta=angle(Z(i));
SL= abs(Spower(i));
Zth=abs(Z(i))
alpha=angle(((v(i))^2)/conj(Spower(i)));
Eth=abs(Vx(i));
%compute PTSI
PTSI=(2*SL*Zth*(1+cos(beta-aplha)))/((Eth)^2);
%load bus PTSI
compPTSI(i,j)=PTSI;
end
end

%*****

%thevequiv() - This Code Computes the Thevenin Parameters
%case:increasing load demand at constant power factor
%14 bus system
function [Vth,Zth,powers,Yx] = thevequiv(casenum)
%m-files input: synchrophasor.m,updateHLG.m
%specify the case for test
[V,S,gens,ybus] = synchrophasor(casenum);

%Partition The Vmatrix Vector
[YLL,YLT,YTT,YTL,YTG,YLG,Y] = updateHLG(gens,ybus);
[r,c]=size(YLL);
uVal = c-8;
VL = V(1:8+uVal);
VT = V(9+uVal);
VG = V(10+uVal:14);
%Partition The Ymatrix
%N = #of load buses
%M = #of source buses
ZLL = (YLL-(YLT*(YTT^-1)*YTL)^-1;
ZLT = -ZLL*YLT*(YTT)^-1
HLG = ZLL * (YLT*(YTT^-1)*YTG-YLG);
%calculate Thevenin Equivalent
for j = 1:8
VN=0;
VM=0;
for i =1:c
if i == j
continue
else
VN=VN+ZLL(j,i)*conj((-S(i))/VL(i));
end
end
for k =10+uVal:14

```

```

VM=VM+HLG(j,k)*VG(k)
end
Veq(j,1)=VN+VM;
Zeq(j,1)=ZLL(j,j);
end
Vth = Veq;
Zth = Zeq;
powers=S;
Yx=Y;

%*****

function [YLL,YLT,YTT,YTL,YTG,YLG,Ybus] =
updateHLG(busnum, syncYbus)
%This code updates the ZLL and HLG Matrix
%Case:increasing load demand at constant power factor
%busnum - the bus number vector to be updated; with x
number of columns
%input:syncbus.m

Ymatrix = syncYbus;
Ybustemp = Ymatrix;
newYbus=Ybustemp;
if busnum == 0
YLL = Ybustemp(1:8,1:8);
YLT = Ybustemp(1:8,9);
YTT = Ybustemp(9,9);
YTL = Ybustemp(9,1:8);
YTG = Ybustemp(9,10:14);
YLG = Ybustemp(1:8,10:14);
Ybus=Ybustemp;
else
[r,c] = size(busnum); %the number of rows and columns.Should
be 1 row
%construct new Ybus
for i=1:c
gencol = Ybustemp(:,busnum(i));
genrow = Ybustemp(busnum(i),:);
selfgen = gencol(busnum(i),1);
genrow(1,busnum) = 0;
if abs(sum(genrow(1:8)))>1
else
genrow = circshift(genrow,[0,i-1]);
end
gencol(busnum,1)=0;
if abs(sum(gencol(1:8)))>1
else
gencol = circshift(gencol,i);

```

```

end
gencol(8+i,1) = selfgen;
newYbus = insertrows(newYbus,genrow,8+i-1);
newYbus(busnum(i)+1,:)=[];
newYbus = insertrows(newYbus',gencol',8+i-1)';
newYbus(:,busnum(i)+1)=[];
end
Y= newYbus;
YLL = Y(1:8+c,1:8+c);
YLT = Y(1:8+c,9+c;
YTT = Y(9+c,9+c);
YTL = Y(9+c,1:8+c);
YTG = Y(9+c,10+c:14);
YLG = Y(1:8+c,10+c:14);
Ybus=Y;
end

%*****

%this code computes VCPI of 14 bus system
%case:increasing load demand at constant power factor
%m file input:synchrophasor.m

Vcpi =0;
for x=1:7
[ymatrix,V] = synchrophasor(x);
indexCreate=0;
Vmpsum =0;
indices = 0;
[r,c] = size(ymatrix);
bus = r;
%get VCPI at bus k
%create Ykj summations
Ykj = 0;
ysum = 0;
for i=1:bus
ysum = 0;
for j = 1:bus
if j ==i
continue
else
ysum = ysum + ymatrix(i,j);
end
end
Ykj(i) = ysum;
end
for k=1:bus
Vmpsum = 0;

```

```

for m = 1:bus
if m == k
continue
else
Vmpsum = Vmpsum + V(m)*ymatrix(k,m)/Ykj(k);
end
end
index(k,1) = abs(1-Vmpsum/V(k));
end
loads=[4,5,9,10,11,12,13,14];
for i =1:8
vcpi(i,x)=index(loads(i),1);
end
end

```

REFERENCES

- [1] **A. G. Phadke**, "Synchronized phasor measurements in power systems," *IEEE Comput. Appl. Power*, vol.6, no. 2, pp. 10-15, Apr.1993.
- [2] **Altuve, Ferrer Hector J., and Edmund O. Schweitzer**. *Modern Solutions for Protection, Control, and Monitoring of Electric Power Systems*. Pullman, Wash. (2350 NE Hopkins Court, Pullman, WA 99163 USA): Schweitzer Engineering Laboratories,2010.Print
- [3] **S. Massucco et al**, "Evaluation of some indices for voltage stability assessment", *IEEE Bucharest Power Tech Conference*, 28th June-2nd July, Bucharest, Romania, pp.1-8.
- [4] **Reis,C.;Barbosa.;F.P.M.**,"A comparison of voltage stability indices". *Electrotechnical Conference, 2006. MELECON 2006. IEEE Mediterranean*, vol., no.,pp.1007,1010, 16-19 May 2006.
- [5] **Cupelli, M.; Doig Cardet, C.; Monti, A.**, "Voltage stability indices comparison on the IEEE-39 bus system using RTDS," *Power System Technology (POWERCON), 2012 IEEE International Conference on* , vol., no., pp.1,6, Oct. 30 2012-Nov. 2 2012
- [6] **Massucco, S.; Grillo, S.; Pitto, A.; Silvestro, F.**, "Evaluation of some indices for voltage stability assessment," *PowerTech, 2009 IEEE Bucharest*, vol., no., pp.1,8, June 28 2009-July 2 2009.
- [7] **Kundur, P., Neal J. Balu, and Mark G. Lauby**. *Power System Stability and Control*. New York: McGraw-Hill, 1994. Print.
- [8] **Taylor, Carson W., Neal J. Balu, and Dominic Maratukulam**. *Power System Voltage Stability*. New York: McGraw-Hill, 1994. Print.
- [9] **P. Kundur et al.**, "Definition and classification of power system stability", *IEEE Transactions on Power Systems*, Vol. 19, No. 2, May 2004, pp. 1387-1401.
- [10] **Pal, M.K.**, "Voltage stability conditions considering load characteristics," *Power Systems, IEEE Transactions on*, vol.7, no.1, pp.243-249, Feb 1992.
- [11] **Glover, J. Duncan., and Mulukutla S. Sarma**. *Power System Analysis and Design*. Boston: PWS Pub., 1994. Print.
- [12] **P. W. Sauer and M. Pai.**, *Power system dynamics and stability*. Prentice Hall, 1998.

- [13] **T. Van Cutsem** and **C. Vournas**, *Voltage Stability of Electric Power Systems*. Norwell, MA: Kluwer, 1998.
- [14] **Yanfeng Gong** and **Noel Schulz**, "Synchrophasor-Based Real-Time Voltage Stability Index", *Proc.Power system Conference and Exposition*, 2006. PSCE'06, IEEE PES, pp. 1029-1036, October 2006.
- [15] **V. Balamourougan**, **T. S. Sidhu**, and **M. S. Sachdev**, "Technique for online prediction of voltage collapse," *IEE Proceedings in Generation, Transmission and Distribution*, Vol. 151, No. 4, July 2004, pp. 453–460.
- [16] **Nizam Muhammad**, **Azad Mohammed** and **AiniHussian**, "Performance Evaluation of Voltage Stability Indices for Dynamic Voltage Collapse Prediction", *Journal of Applied Sciences*, Vol. 6, no. 5, pp. 1104-1113, May 2006.
- [17] **J. Depablos**, **V. Centeno** et al, "Comparative testing of synchronized phasor measurement units", *IEEE Power and Energy Society General Meeting 2004*, June 2004, pp. 948-955.
- [18] **M. Glavic** and **T. Van Cutsem**, "Wide-area detection of voltage instability from synchronized phasor measurements. Part I: Principle," *IEEE Transactions on Power Systems*, Vol. 24, No. 3, August 2009, pp. 1408-1416.
- [19] **A.Monticelli**, **S. Deckmann**, **A. Garcia**, and **B. Scott**, "Real-time External Equivalents for Static Security Analysis," *IEEE Transactions on Power Apparatus and Systems*, Vol. PAS-98, No. 2, March 1979, pp.498–503.
- [20] **Ken Kato**, "External Network Modeling – Recent Practical Experience," *IEEE Transactions on Power Systems*, Vol. 9, No. 1, February 1994, pp. 216–225.
- [21] **R. R. Shoults** and **W. J. Bierck, Jr.** "Buffer system selection of a steadystate external equivalent model for real-time power flow using an automated model for analysis procedure," *IEEE Transactions on Power Apparatus and Systems*, Vol. 3, No. 3, August 1988, pp. 1104–1111.
- [22] **Li, W.; Wang, Y.; Chen, T.**, "Investigation on the Thevenin equivalent parameters for online estimation of maximum power transfer limits," *Generation, Transmission & Distribution, IET*, vol.4, no.10, pp.1180,1187, October 2010.
- [23] **Allan Agatep**. "Voltage stability Analysis using simulated Synchrophasor Measurements" May 2013
- [24] **De La Ree, J.; Centeno, V.; Thorp, J.S.; Phadke, A.G.;** "Synchronized Phasor Measurement Applications in Power Systems", *Smart Grid, IEEE Transactions on*, vol.1, no.1, pp.20-27, June 2010.

- [25] **Zakir Hussain Rather., Zhe Chen., Paul Thogersen.,;** “Wide Area based Security Assessment and Monitoring of Modern Power System: A Danish Power System Case Study”, *IEEE ISGT Asia* 2013.
- [26] **Rohikaa Micky R., Lakshmi R., Sunitha R., Ashok S.;** “Assessment of Voltage Stability in Microgrid”, *International Conference on Electrical ,Electronics and Optimisation techniques(ICEEOT)*-2016